Fluorescently Conjugated Annular Fibrin Clot for Multiplexed Real-time Digestion Analysis

Ziqian Zeng [a,b], Tanmaye Nallan Chakravarthula [a,b], Charanya Muralidharan [c,d], Abigail Hall [a], Amelia K. Linnemann [c,d], Nathan J. Alves [a,b,c*]

[a] Department of Emergency Medicine, Indiana University School of Medicine, Indianapolis, IN
[b] Weldon School of Biomedical Engineering, Purdue University, West Lafayette, IN
[c] Department of Biochemistry & Molecular Biology, Indiana University School of Medicine, Indianapolis, IN
[d] Department of Pediatrics, Indiana University School of Medicine, Indianapolis, IN

[*] Corresponding author:
Nathan J. Alves, PhD
Indiana University School of Medicine
635 Barnhill Dr. Rm. 2063
Indianapolis, IN 46202, United States of America
E-mail address: nalves@iu.edu (N.J. Alves).

Abstract
Impaired fibrinolysis has long been considered as a risk factor for venous thromboembolism. Fibrin clots formed at physiological concentrations are promising substrates for monitoring fibrinolytic performance as they offer clot microstructures resembling *in-vivo*. Here we introduce a fluorescently labeled fibrin clot lysis assay which leverages a unique annular clot geometry assayed using a microplate reader. A physiologically relevant fibrin clotting formulation was explored to achieve high assay sensitivity while minimizing labeling impact as fluorescence isothiocyanate (FITC)-fibrin(ogen) conjugations significantly affect both fibrin polymerization and fibrinolysis. Clot characteristics were examined using thromboelastography (TEG), turbidity, scanning electron microscopy, and confocal microscopy. Sample fibrinolytic activities at varying plasmin, plasminogen, and tissue plasminogen activator (tPA) concentrations were assessed in the present study and results were compared to an S2251 chromogenic assay. The optimized physiologically relevant clot substrate showed minimal reporter-conjugation impact with nearly physiological clot properties. The assay demonstrated good reproducibility, wide working range, kinetic read ability, low limit of detection, and the capability to distinguish fibrin binding-related lytic performance. In combination with its ease for multiplexing, it also has applications as a convenient platform for assessing patient fibrinolytic potential and screening thrombolytic drug activities in personalized medical applications.

Keywords: FITC-fibrin(ongen), thrombosis, plasmin, clot lysis, fibrinolytic potential

---

This is the author's manuscript of the article published in final edited form as:

Zeng, Z., Nallan Chakravarthula, T., Muralidharan, C., Hall, A., Linnemann, A. K., & Alves, N. J. (2021). Fluorescently conjugated annular fibrin clot for multiplexed real-time digestion analysis. Journal of Materials Chemistry. B, 9(45), 9295–9307. https://doi.org/10.1039/d1tb02088a

Highlights:

- Fluorophore conjugating fibrin(ogen) largely disrupt fibrin clot properties.
- Conjugation impact can be minimized by diluting labeled fibrinogen with fibrinogen.
- Annular clot geometry can facilitate kinetic clot lysis monitoring and multiplexing.
- Labeled annular clot assay can distinguish fibrin-binding related lytic activity.

1. Introduction

Impaired fibrinolysis has long been considered a risk factor for venous thromboembolism (VTE). Although efforts have been made over the years, no existing fibrinolytic assessment assays appears to genuinely aid in thrombosis diagnosis or offer a reliable testing platform for therapeutic development [1–3]. In response to blood vessel injury, the human body initiates a hemostasis process which is an innate series of actions ultimately resulting in clot formation. Fibrin is a protein that is primarily responsible for clotting and degrades through a fibrinolysis process that following hemostasis. A typical fibrinolysis process involves the activation of plasminogen by tissue plasminogen activator (tPA) to produce plasmin, which is the enzyme that is responsible for fibrin digestion. The five kringle domains present on the surface of plasmin bind to C (carboxy)-terminal lysine residues on fibrin to facilitate local clot binding and subsequent digestion via its catalytic domain. The fibrinolytic system is carefully regulated by inhibitors including type 1 plasminogen activator inhibitor (PAI-1) which regulates tPA activity in addition to α2-antiplasmin and α2-macroglobulin which regulate plasmin activity [4–6]. In acute thrombosis patients, thrombolytic drugs known as recombinant plasminogen activators can be administered to accelerate plasmin conversion and clot digestion to offer a fast relief from life-threatening clotting events such as pulmonary embolism and ischemic stroke [7–9]. Despite the development of novel drug agents, the clinical translation success rate remains very low in part due to a lack of representative drug testing platforms. Due to the complexity of the fibrinolytic system, an ideal fibrinolytic testing platform for diagnosis and drug development applications should use a standardized substrate and be capable of dynamically monitoring the fibrinolytic process at a physiologically relevant scale and offer reproducible and translatable results.

Numerous assays have been developed to meet this challenge, but all exhibit a variety of benefits and drawbacks limiting their overall utility. Chromogenic or antigenic assays are frequently used to measure individual clotting factor levels or activities. These assays, however; do not directly yield clinically representative results as they are unable to assess processes that involve native fibrinolytic events such as protein adsorption, multi-factor interactions, or plasmin-fibrin binding. Assays such as euglobulin clot lysis time (ECLT) and dilute whole-blood clot lysis time (DWBCLT), have been extensively used since the 1980s [1,10,11]. While these assays more globally represent *in-vivo* clotting conditions they are inherently difficult to measure an accurate plasma fibrinolytic activity as they either test only a small sub-fraction of plasma or ignore the presence of varying amounts of fibrinogen in the test system. More recently, a plasma clot lysis assay was developed that tracks clot turbidity, an optical measure of bulk clot structure, over time. It has rapidly gained popularity for use in clinical studies due to its ease of implementation [12–14]. Using tissue factor and tPA-treated patient plasma, a change in clot turbidity is monitored throughout the clot formation and lysis processes. However, this assay utilizes the patient's own plasma and

results are often difficult to compare across samples due to variations from patient-to-patient. For example, clot lysis time is influenced by fibrinogen levels due to its impact on fibrin clot formation density and fiber thickness making interpretation of therapeutic effect by turbidity difficult [2]. More importantly, the turbidity reading lacks microstructural or molecular interpretation capabilities. Although a fibrin fiber mass-length ratio can be extracted from turbidity measurements, the calculation relies on a number of assumptions that are sometimes difficult to determine [15]. None of these assays allows for a physiologically relevant clot lysis determination that provides results than can directly be compared across patients in the presence and absence of a variety of therapeutic interventions.

Additional assays utilize exogenous fibrin as the substrate to assess fibrinolytic activity with the ability to offer physiologically relevant microstructures including binding moieties, cleavage sites and clot digestion depths. The fibrin plate method measures fibrinolytic potential by quantifying the lysed area of preformed fibrin in a petri-dish following incubation with a drop of patient plasma to its center. The assay is difficult to multiplex, and quantification methods require standardization to allow for comparison across groups [16]. Radioactively or fluorescently labeled fibrin clot lysis assays have also been developed to measure plasmin activity or plasma fibrinolytic potential [17,18]. These assays incorporate molecular reporters such as ^{125}I or fluorescein isothiocyanate (FITC) labels in preformed fibrin clots to track clot digestion activity. Fibrinolysis is monitored by tracking the reporter signal released into the clot supernatant during digestion. The monitored fibrinolytic activity is independent of fibrinogen concentration in patient samples [19]. A common setup of such assays requires the frequent transfer of clot supernatant to a clean well for signal acquisition throughout the digestion process making these assays intensive and lacking the ability for dynamic reads over time without disturbing the assay. This procedure largely interferes with the ongoing fibrinolytic reaction, introducing artifacts and making it difficult for multiplexing, standardization, and utilization under fast-responding clinical interventions. More importantly, both isotopic iodine and FITC molecules conjugate fibrinogen none-specifically at primary amines of lysine residuals. These conjugations are irreversible and can negatively impact the fibrin polymerization process resulting in disrupted fibrin structures [20]. When conjugations block C-terminal lysine residuals, or alternate digestion sites on fibrin, fibrinolysis becomes less representative as a constant exposure of these residuals is critical [21,22]. Therefore, results of these assays may not have good clinical relevance unless a characterization of reporter-labeled fibrin clots is thoroughly addressed.

This study describes a highly reproducible *in-vitro* clot lysis assay that offers a physiologically relevant assessment of sample fibrinolytic activity through a controlled fibrin substrate and easily multiplexed design. The assay utilizes a FITC-labeled fibrin-based clot forming at physiological fibrinogen and thrombin concentrations. The clot substrate was engineered to be an annular shape and pre-formed in a 96-well plate with the help of a 3D-printed molding insert. Specifically, the unique clot geometry provides for a clear light path for fluorescence excitation and emission by taking advantage of the centrally located signal acquisition mechanism of a commercial spectrometer (Figure. 1). With the addition of fibrinolytic sample solution to the center of the annular clot, increasing amounts of soluble fluorescently tagged fibrin degradation products are released and measured dynamically over time. These fragments disperse into the solution and fluorescence signal is monitored by the detector. This setup enables a real-time measurement of clot lysis with no disturbance during the reading process. To reduce FITC-fibrin(ogen) conjugation

impact on clot formation/digestion and to establish a physiologically relevant FITC labeled clot, clotting mixtures using different FITC per fibrinogen and different ratios of FITC-fibrinogen to unmodified fibrinogen were explored. Multiple tools were used to assess fibrin clot characteristics. Clot formation, bulk structure and viscoelastic property were examined by clot turbidity and thromboelastography (TEG) assays. Clot microstructure, including fiber thickness and pore size, was examined via scanning electron microscopy (SEM). Fluorescence labeling homogeneity and signal density were compared via confocal microscopy. This information was combined to guide an optimized FITC labeling strategy in fibrin to achieve a physiologically relevant FITC labeled fibrin clot that is structurally indistinct from an unmodified *in-vitro* statically formed fibrin clot. The FITC-fibrin clots were further tested for fibrinolysis using samples that contain plasmin, or a mixture of exogenous tPA and plasminogen, to demonstrate the assay's capacity of differentiating sample fibrinolytic potential or examining drug dose-response.

2. Experimental

2.1 FITC-fibrinogen conjugation

Human fibrinogen and thrombin lyophilized powder (Sigma Aldrich, St. Louis, MO) were reconstituted in phosphate buffer saline (PBS) and deionized water (DI), respectively. FITC (Sigma Aldrich, St. Louis, MO) was reconstituted in PBS with 10% dimethyl sulfoxide (DMSO) to improve solubility. FITC labeled human fibrinogen (FhF) is made by mixing 200-fold excess FITC to fibrinogen at room temperature (RT) in PBS for 10, 120 minutes, and overnight to attain three different FITC per fibrinogen labeling levels (<8% DMSO in reaction solution). Following conjugation, tagged fibrinogen was purified from unreacted FITC using serial dilutions in 100 kDa molecular weight cutoff centrifugal filters following manufacturer recommendations (Amicon®, Millipore, Burlington, MA). The number of FITC per fibrinogen were determined to be 3, 7, and 12- FITC per human fibrinogen comparing 280 and 494nm absorptivity via a spectrometer (Molecular Device® SpectraMax M5, San Jose, CA), calculated through Beer's law and molar extinction coefficients, $\varepsilon = 513,400$ L mol^{-1} cm^{-1} (at 280 nm) for fibrinogen and $\varepsilon = 75,855$ L mol^{-1} cm^{-1} (at 494 nm) for FITC. FITC absorbance contribution at 280 nm was subtracted. FhFs were aliquoted and stored at -20 °C and thawed directly before experiments. These FhF products were experimentally found to be active for clot formation and stable with no change in absorbance (280 nm and 494 nm) or fluorescence intensity for four consecutive freeze-thaw cycles and over a period of four weeks of storage (Suppl. Fig. 1).

2.2 Clotting solution preparation

Unmodified fibrinogen was mixed with 3, 7, 12-FhF at fibrinogen to FhF ratios of 1:0 (unmodified fibrinogen control), 5:1, 10:1, 30:1, 50:1, and 0:1 (neat FhF). All fibrin clots were formed at a final concentration of 3 mg/mL fibrinogen and 1U/mL thrombin in PBS.

2.3 FITC-fibrin turbidity and TEG assays

Clot characterization via clot turbidity and TEG assays were described previously [23,24]. Clot turbidity assays were initiated by mixing thrombin with fibrinogen in a 96-well plate (Corning®, Corning, NY) and monitored at 550 nm absorbance for 30 min via a spectrometer. $Turb^{max}$ (maximum turbidity) was derived from the turbidity tracing curve. TEG assays were initiated by mixing thrombin with fibrinogen in a clear TEG cup and monitored for 30 min in a TEG 5000 Analyzer (Haemonetics®, Braintree, MA). TEG^{max} (maximum amplitude or MA) was derived by the TEG software (Haemonetics®, Braintree, MA).

2.4 Scanning Electron Microscopy

Fibrin clots (80 µL) were fixed by 2.5% glutaraldehyde (Electron Microscopy Sciences Supplier, Hatfield, PA) in PBS solution overnight and washed with DI water five times. Clot samples were then fully dehydrated via overnight lyophilization (FreezeZone 2.5, Labconco). It is important to note that the fibrin dehydration process was critical to preserve its micro-morphology under SEM since clots formed in this study were at a concentration of only 0.3% (w/v). Additional dehydration methods were also assessed (Suppl. Fig. 2). Dehydrated samples were further sputter coated with gold (Denton Vacuum Desktop V) for 30 seconds at $3*10^{-4}$ Torr to obtain a ~ 10 nm gold coating for SEM. Fibrin micro-structural images were taken using a field emission scanning electron microscopy (JSM-7800F, JEOL) at an acceleration voltage of 5 kV. Fiber diameters, pore size, pore counts, and total pore area were quantified using an open-source Image J software.

2.5 Confocal microscopy

Selected fibrin clots were prepared in a 35 mm glass-bottom dish (MaTek Corporation) microscope dish at a volume of 40 µL. Images were acquired using LSM 800 confocal microscope (Zeiss, Germany) equipped with a C-Apochromat 40X/1.20W Korr objective. FITC was excited at 488 nm and collected at 519 nm (maximum emission). Confocal fluorescence images were analyzed using Image J.

2.6 Fibrin clot stability after storage

FITC-Fibrin clots and unmodified fibrin clots were formed in a 96-well plate at 150 µL and stored at RT and 4 °C for comparison. Longitudinal fibrin clot stability was tested by tracking turbidity at 550 nm over 56 days.

2.7 Annular clot fabrication

The annular clot molding insert was designed and drafted using an open-source CAD software based on dimensions of a UV transparent 96-well plate (Corning® 3635). The insert was 3D printed at the IU Health 3D Innovations Lab using a Stratsys® Connex 3 printer (Figure. 1A) providing for high precision with a build layer as fine as 16 µm. The body of the insert used an acrylic-based material (VeroClear® RGD810) to ensure a smooth surface. The elastomeric end cap (TangoPlus® FLX930) was later cured at the end of the insert to prevent unwanted clot formation in the light path at the base of the well. Annular clots were formed by directly adding clotting solution to the plate at 80 µL and immediately placing the DI water rinsed 3D printed insert into the well. The insert was gently pressed during the first 2 min to ensure a good bottom seal. After 30 min clotting at RT the insert was carefully removed, and the annular clots were gently washed with 0.01 M PBS twice and stored in 120 µL PBS before use.

2.8 Dose response experiment

Lyophilized plasmin, plasminogen (Athens Biotech, Athens, GA) and tPA (Alteplase® Genentech, San Francisco, CA) were reconstituted in DI water. Sample solutions were made by diluting stock to targeted concentrations with PBS. Plasmin dose-response experiments were conducted at 0.01 to 1.5 U/mL unless otherwise specified. For experiments with varying plasminogen and fixed tPA level (500 ng/mL), 0 to 87.2 µg/mL plasminogen were examined. For experiments with varying tPA and fixed plasminogen level (58.1 µg/mL), 0 to 1000 ng/mL tPA were examined.

2.9 Annular clot lysis assay

In all experiments, 120 µL sample solution was well mixed and added to the center of the annular clot to initiate clot lysis. Fluorescence (Ext 495, Em 519) was monitored for 60 min at a 30 sec interval without pre- or post- shaking. Shaking can be added to improve mixing but was not necessary for efficient assay progression. All clot lysis experiments were performed at 37 °C in triplicate. The Limit of Detection (LoD) is defined as the lowest analyte concentration reliably distinguished from the blank. Thus, LoDs of annular clot lysis assay were determined based on the measured Limit of Blank (LoB) and the lowest concentration of plasmin that has a significantly different fluorescence release rate compared to the blank. Analytical sensitivity was determined by the slope of a linear fitted line at lower plasmin concentrations (<0.05 U/mL) [25].

2.10 S2251 chromogenic assay

S2251 assays were performed in non-binding 96-well plates (Corning® 3641). Sample solutions were pipetted into the well containing 500 µM S2251 chromogenic substrate (Diapharma, West Chester, OH) at a final volume of 100 µL. p-Nitroaniline (pNA) absorbance (405 nm) was monitored for 10 min at a 30 sec interval. All experiments were performed at 37 °C with experimental groups in triplicates. V_0 (Initial velocity) was derived using the initial linear region of the absorbance tracing curve.

2.11 Statistical Analysis

All results were reported as mean ± standard deviation. Two tailed student t-tests were performed, and significant statistical differences were reported at P values < 0.05. P values lower than 0.01 and 0.001 were also indicated as appropriate in plots and tables. Linear regressions were fitted in some plots and corresponding R^2 values were reported. The detailed protocols were specified in corresponding figure legends.

3. Results and Discussion

3.1 Effect of Fibrinogen Tagging on Clot Formation

The clinical relevance of an *in-vitro* fibrin clot lysis assay relies on a representative clot substrate that has non-disrupted physical and biological properties. Since the FITC-fibrinogen conjugation is mediated through a covalent bond, it is necessary to examine the fibrinogen tagging effect on clot properties. In this study, FITC labeled human fibrinogen (FhF) was made by incubating human fibrinogen with FITC at a 200-fold excess. Although a single fibrinogen molecule has around 200 lysine residues, we can only achieve a maximum of 16 FITC per fibrinogen. FITC conjugation sites on fibrinogen were also identified (Figure. 2A) and detailed in Suppl. Fig. 3 and 4. By increasing the incubation time from 10 min to 2 hours to overnight, 3, 7, and 12- FITC per fibrinogen were fabricated and these numbers were determined via spectrometer using 494 nm to 280 nm absorbance conversion derived from the FITC absorbance spectrum. To assess the effects of fibrinogen tagging on fibrin clot formation, FhF were mixed with unmodified fibrinogen prior to thrombin initiated fibrin formation (Figure. 2B). Bulk clot strength and fibrin fiber packing were examined by TEG and turbidity assays. Turbidity and amplitude were tracked over time for clots formed at increasing levels of FITC-fibrinogen (Figure. 2C and 2D). $Turb^{Max}$ and TEG^{Max} were obtained for analysis and data were normalized to that of unmodified human fibrinogen to eliminate batch-to-batch variation (± 9% for $Turb^{Max}$ and ± 5% for TEG^{Max}) and allow for direct comparisons of percent change across samples. All tested sample turbidities were within the detection limit of the spectrometer and were baseline-subtracted before data normalization. FITC

absorbance at 550 nm at the concentrations used in this study are negligible. As was expected, FITC-fibrin(ogen) conjugation rendered a significant impact to both clot strength and macroscopic clot structure as determined by turbidity. Overall, increasing FhF levels (FhF to fibrinogen ratio) in the clot contributed to higher $Turb^{Max}$ (maximum turbidity) and lower TEG^{Max} (clot strength) which was consistently observed in all three groups (3, 7 and 12-FhF) (Figure. 2E and 2F).

Specifically, neat 3, 7 and 12-FhF clot samples showed 45, 74 and 92% reduction in clot strength and 35, 65, and 69% increase in clot turbidity compared to unmodified fibrinogen, respectively. 12-FhF showed very low TEG^{Max} and high $Turb^{Max}$ amidst all neat samples indicating a larger disruption of fibrin polymerization due to an increase of FITC-conjugations per fibrinogen. At lower FhF ratios, clot strength and clot turbidity values leveled off and matched values of the unmodified fibrinogen sample. The inverse tracking of clot strength and clot turbidity at increased FhF ratios in fibrin resembled what was observed in experiments on varying multiple other clotting variables published previously [23]. Importantly, this combination of high turbidity and low clot strength at a constant fibrinogen level demonstrates formation of thick fibers and a loose fibrous fibrin network. Time to maximum clot strength was also determined to assess the impact of fibrinogen tagging on the dynamic process of clotting (Suppl. Fig. 5). Under both assays, most samples showed a similar time to maximum clot formation with a difference less than 20% indicating similar clotting performance across groups. However, neat 12-FhF sample showed three times longer time to achieve maximum clot strength compared to all other samples due to its slow clotting progression and low ultimate clot strength.

From this analysis, physiologically relevant fibrin clotting mixtures for each of the modified fibrinogen levels were determined through matching clot properties of a sample to that of the unmodified fibrin clot. Therefore, 7FhF (30:1) and 12FhF (50:1) groups were determined to be physiologically relevant as their $Turb^{Max}$ and TEG^{Max} showed no statistical difference ($P < 0.05$) above 30:1 and 50:1, respectively. 3FhF (10:1) was also selected as a physiologically relevant mixture as TEG^{Max} showed no statistical difference while $Turb^{Max}$ showed less than 10% difference.

3.2 Fibrin clot Morphology via SEM

To directly assess clot morphology at varying ratios of tagged and untagged fibrinogen, SEM was carried out on an array of fibrin clot mixtures. These clots include neat FhF, unmodified fibrin clots, and three physiologically relevant FhF clot samples--3FhF (10:1), 7FhF (30:1) and 12FhF (50:1). Clots were formed, crosslinked, lyophilized and gold coated prior to SEM analysis. Clot microstructures were compared at 4,000X and 35,000X magnifications (Figure. 3A and 3B).

Neat FhF clot samples exhibited scale-like patterns and fused fibrin fiber morphology. These clots were further categorized as having larger fiber diameter, smaller pore size and smaller total pore area percentage compared to the other groups (Figure. 3C). A quantitative analysis was conducted using Image J. Pore size and total pore area were measured using a thresholding method where the same threshold level was applied across all the samples throughout the analysis. Based on the quantitative results, the neat 12FhF clot sample showed the most unique and dissimilar SEM morphology, i.e., thickest fiber and lowest pore area. These direct morphological measurements are consistent with the bulk clot structure as assessed by clot turbidity. The physiologically relevant clot groups showed much cleaner fibrin morphology more similar to that of neat unmodified fibrinogen clots.

Despite having similar TEG and turbidity values as unmodified fibrinogen, not all physiologically relevant groups exhibited a native fibrin structure under SEM. 3FhF (10:1) and 7FhF (30:1) clots showed similar fiber diameters compared to unmodified fibrin clots but both groups were found to have significantly smaller pore size and a moderate level of fused fibrin fiber morphology. Only the 12FhF (50:1) sample showed minimal differences, both qualitatively and through defined characteristics, compared to the unmodified fibrin control. This suggests that the ratio of fibrinogen to FhF rather than the amount of FITC per fibrinogen exerts a larger ultimate impact on fibrin structure upon clotting. To further explore this, the effect of fibrinogen to FhF ratio on clot micro-morphology was further examined under SEM. In this experiment, clots were formed by decreasing 12FhF ratios (fibrinogen to FhF = 0:1, 10:1, 30:1, 50:1, 1:0) in the fibrin (Suppl. Fig. 6 and Suppl. Table. 1). Results showed that the presence of more FhF contributed to clots with significantly larger fiber diameters, reduced pore size and total pore area. This confirmed that increasing FITC-fibrin(ogen) levels in fibrin clots disrupt clot properties resulting in less physiologically relevant fibrin clots. In summary, the clotting solution that mixes unmodified fibrinogen with 12 FITC per human fibrinogen at 50:1 ratio produces the most physiologically relevant fibrin clot as determined by TEG, Turbidity, and SEM.

3.3 Tagging Consistency via Confocal Microscopy

Homogeneity of FITC incorporated into the final fibrin clot structure is critical to ensure that release of FITC during clot digestion is consistent throughout the entirety of the clot digestion process. To assess FITC labeling homogeneity, z-stack confocal images of neat and physiologically relevant 3, 7, 12FhF formed fibrin samples were taken at three different locations with five slices at an interval of 10 μm. Three slices at locations that are 30 μm below the surface were used for comparison and quantitative analysis. Neat FhF clot samples exhibit bright images with significant fluorescent aggregates at higher FITC per fibrinogen whereas the three physiologically relevant FhF clots showed homogeneous FITC labeling throughout their fibrin structures (Figure. 4A and 4C). Unmodified fibrin clots could not be imaged utilizing this technique as they did not exhibit endogenous fluorescence in the absence of FITC tagging.

Neat and physiologically relevant FhF clot samples were excited at 0.2% and 1% energy levels to avoid signal underexposure or saturation, respectively. Images were taken immediately after excitation to avoid photobleaching over time. Integrated intensities were reported in fluorescence units (FLU, or arbitrary units) per μm^2 by averaging multiple images at different depths for each sample in bar plots (Figure. 4B and 4D). It was not surprising that neat FhF clots showed higher integrated intensity at increased FITC per fibrinogen. However, the value of the neat 12FhF sample is only 1.5 times as that of the neat 3FhF sample while the FITC concentration ratio of these two samples is 4 times higher. This represents a reduction in intensity per FITC of 62% indicative of local fluorescence quenching due to increasing FITC proximity on fibrinogen which has been reported previously [18,26]. Comparing 12FhF (50:1) to 3FhF (10:1) samples, integrated intensity ratios and FITC concentration ratios were also mismatched contributing to a 64% reduction of integrated intensity per FITC in the former group. 7FhF neat and 7FhF (30:1) samples also showed 39.6% and 42.7% reductions in integrated intensity per FITC compared to 3FhF neat and physiologically relevant samples, respectively. Since similar levels of reduction in integrated intensity per FITC were observed for neat and physiological relevant samples, fluorescence quenching was dominated by intra-fibrinogen quenching effects rather than inter-fibrinogen

quenching. This quenching effect is largely due to the use of FITC as a fluorescent probe and can be mitigated by selecting a probe that is less prone to self-quenching.

The labeling homogeneity was quantitatively assessed by looking at the integrated intensity fluctuation across a set of five image locations. All neat FhF samples showed > 20% fluctuation in fluorescence intensity with obvious fluorescence aggregation while physiologically relevant FhF samples exhibit less than 10% variation. This confirmed that physiologically relevant FhF samples have a more consistent labeling homogeneity throughout the clot. Additionally, the unlabeled area between the fluorescently labeled fibers were also quantified using a thresholding method in Image J. The unlabeled area is a function of both empty space in the clot, and fluorescent labeling density. While the physiologically relevant clot samples shared similar clot structure under SEM, the 3FhF (10:1) showed 63.0% ± 1.1% unlabeled area which is significantly lower than 76.2% ± 6.7% ($P < 0.001$) for 7FhF (30:1) and 80.9% ± 7.2% ($P < 0.001$) for 12FhF (50:1). This result was expected due to physiologically relevant 3FhF clot sample having the highest labeling ratio of 10:1, representing the most total FITC in the clot of any of the physiological ratios. Based on clot characterization results from clot turbidity, TEG, and SEM, 12FhF (50:1) showed the best match to unmodified fibrin. Although its fluorescence labeling signal intensity was not the highest via confocal microscopy among all three physiological relevant formula, the 12FhF (50:1) clotting mixture demonstrates good labeling homogeneity which potentiates a uniform tracking of fluorescence signal during subsequent clot lysis experiments in the annular clot digestion assay.

3.4 Annular Clot Formation

Fluorescently labeled fibrin digestion cannot be monitored directly through the labeled clot substrate to track clot digestion due to the saturating level of fluorescent tag present in the excitation path. A common solution to this saturation problem is to allow digestion to proceed for a short period of time before removing, or sampling, the digestion supernatant to take static reads throughout the digestion process. This procedure prevents real-time clot digestion tracking and removing of clot supernatant disrupts the clot digestion process negatively impacting assay reproducibility and limiting the capability to multiplex the assay.

The annular clot geometry described herein is a simple and unique solution to the problem of real-time clot lysis monitoring. Through utilizing commonly available 3D printing technology, a small plastic insert can be fabricated for use in a 96-well plate assay format (Figure. 1). This design not only enables real-time signal tracking through measuring soluble digestion fragments that enter the vacant interior of the annular clot, but it also increases assay-multiplexing potential and largely eliminates experimental artifacts commonly associated with repeat sampling type assays. As determined from the characterization experiments in the previous sections, the 12FhF (fibrinogen to FhF=50:1) was selected as the clotting mixture to form the physiologically relevant FITC-fibrin clots. The annular clots were made by placing the insert into the clotting mixture directly following clot initiation through mixing thrombin with neat or physiologically relevant 12FhF solutions. Following 30 minutes the molding insert can be removed and due to the smooth walls of the insert no visible interruption to the annular clot surfaces can be seen following removal. The inserts can be reused indefinitely. The annular clot showed an average volume of 60.5 ± 0.8 μL and an averaged background value of 798 ± 319 fluorescence unit ($n = 114$). With the addition of PBS into the center of the annular clot, no degradation of fibrin was observed throughout the duration

of the experiments as determined by monitoring absorbance at 280 nm. Overall, the described annular clot method is a highly reproducible elegant solution to a common problem with far reaching potential to have an impact in the field of drug development and as a diagnostic tool in the areas of coagulation and fibrinolysis.

3.5 Effects of Fibrinogen Tagging on Plasmin Clot Digestion

Plasminogen is the protease present in the blood plasma primarily responsible for fibrinolysis following activation into its active plasmin form. Its activity directly contributes to the fibrinolytic potential of a plasma sample. Maximal inducible plasmin activity in plasma is about 1 U/mL following full activation of endogenous plasminogen and exhaustion of plasmin inhibitors [27]. To examine the fibrinogen tagging effect on fluorescently labeled fibrin clot digestion, increasing amounts of active plasmin were tested comparing S2251 chromogenic substrate to neat 12FhF and 12FhF (50:1) annular clots. In the S2251 assay, the plasmin dose-response result was reported by plotting the initial velocity V_0 (Abs/min) over plasmin concentrations (Figure. 5A). A linear relationship was observed between V_0 and plasmin concentration. At plasmin levels above 1 U/mL the substrate digestion rate occurs too rapidly to get an accurate initial velocity by the spectrometer. In all, the S2251 assay showed good linearity with increasing plasmin levels from 0.01 to 1 U/mL.

Unlike digesting evenly mixed, small soluble peptide substrates like S2251, plasmin digestion of thick and insoluble physiologically relevant fibrin, such as is present in the annular clot format, involves solid-liquid phase interactions and molecular transport. Initial velocity measurements that are commonly utilized for monitoring chromogenic assays need to be modified when applied to the annular fibrin clot lysis assay. Contrary to initial linear signal tracing monitored for S2251 digestion, annular clot lysis assays demonstrate an initial lag phase followed by a linear phase and an ultimate plateau phase (Figure. 6A). The lag phase is associated with plasmin diffusion due to the static nature of the assay and the discrete liquid-solid separation. The diffusion of plasmin is not solely based on its relative hydrodynamic size compared to the fibrin pore size but rather it is also dependent on plasmin-fibrin binding which is achieved through binding of plasmin's kringle domains to fibrin [28]. Recent *in-vitro* experiments have confirmed that diffusion of plasmin(ogen) is restricted within a thin fibrin layer (5-8 μm) due to fibrin bindings [29]. A potential co-contributor to the lag phase is the gradual exposure of more binding sites, i.e., C-terminal lysine residues, by plasmin accumulation to the digestion front [30]. The exposing rate can be easily affected by protease concentration and the presence of protease inhibitors. In the annular clot lysis assay, the lag phase is useful to examine the initial interactions of the protease and fibrin. Taking this into account a new digestion parameter was developed, FLU200, defined as the time it takes to digest enough FhF to reach 200 fluorescence units. At increasing plasmin levels, FLU200 times showed a decreasing trend (Figure. 6B). In the linear phase where fibrin binding moieties are relatively abundant, digestion rate better reflects the maximal fibrinolytic activity of the sample. Therefore, V_{FR} (fluorescence release rate, FLU/min) was derived by taking the maximum velocity (10 min period) to represent clot digestion rate in this assay. Fluorescence signal was tracked over time at a 30 second interval exhibiting an overall faster fluorescence release at a higher plasmin concentration. At lower plasmin concentrations (<1 U/mL plasmin), although lag and linear phases can hardly be distinguished since C-terminal lysine residuals are constantly larger than plasmin amount, digestion rates were still determined at the fastest 10-min linear period. The coefficients of variance were 9.4% for V_{FR} and 10.6% for FLU200 of physiologically relevant 12FhF annular clot digested by 1 U/mL plasmin through experiments performed two weeks apart. Despite the

relatively small coefficient of variance for V_{FR} and FLU200, a standard plasmin calibration curve is recommended prior to testing samples to further reduce clot formation and digestion variation.

Neat and physiologically relevant 12FhF mixtures were compared in the annular clot lysis assay to determine the fibrinogen tagging effects on fibrinolysis. Overall, both annular clot lysis assays showed that V_{FR} increased and leveled off at higher plasmin concentrations, which agreed with clot digestion at increased plasmin as previously described by the fibrin plate method [31]. To derive simple calibration equations to determine plasmin activity in unknown samples, the V_{FR} and plasmin concentrations were plotted in a double-logarithmic scale (Figure. 5B). Data points of both groups showed good linear regressions with $R^2 > 0.95$. Neat and physiologically relevant 12FhF groups shared similar slopes indicating a comparable dose-response performance across tested plasmin concentrations. The analytical sensitivity of the neat 12FhF substrate is 19 times higher than its physiologically relevant counterpart (Figure. 5C). Its LoD was also slightly lower giving a 0.0015 U/mL comparing to 0.0069 U/mL for the physiologically relevant 12FhF clot. The digestion performance of both substrates was further compared using equivalent fibrin degradation rates (V_{FDR}). V_{FDR} of physiologically relevant and neat 12FhF were normalized to absolute FITC quantity by multiplying their V_{FR} values by 50 and 1, respectively. It was anticipated that neat FhF clots would have larger V_{FDR} at these plasmin concentrations since fibrin composed of thick and loose fibers usually exhibit faster clot digestion. Contrary to this prediction, V_{FDR} of physiologically relevant 12FhF clots were 16 to 22 times faster than those of neat 12FhF clots at the tested plasmin concentrations (Figure. 5D). The increased FhF levels impaired fibrinolysis to a large extent. In all, despite the higher levels of signal associated with the neat 12FhF, its digestion was considerably slower than the physiologically relevant 12FhF clots. This reduced digestion rate can be attributed to the tagged fibrin impairing plasmin's ability to bind and facilitate fibrin digestion. For applications in which the highest clot digestion signal is necessary, the neat 12FhF can be utilized. For applications requiring a physiologically relevant clot substrate, preparing a 12FhF (50:1) mixture is necessary.

3.6 Varying Plasminogen and tPA levels on Annular Clot Digestion

In plasma, tPA cleaves plasminogen into plasmin to initiate fibrinolysis. The baseline concentration of plasma tPA is less than 10 ng/mL for healthy individuals.[32] A typical thrombolytic therapy for a pulmonary embolism patient is a regimen of 100 mg Alteplase over 2 hours of intravenous infusion.[33] The catalytic efficiency of plasminogen activation by tPA has been reported to be orders of magnitude higher in the presence of fibrin than in its absence. The S2251 assay has commonly been used to assess urokinase and streptokinase-initiated plasminogen activation but lacks the ability to examine plasminogen activation by tPA due to the absence of fibrin in the assay. To demonstrate a benefit of using the annular clot lysis assay over this chromogenic substrate, digestion solutions made by combining tPA and plasminogen were tested in the physiologically relevant 12FhF annular clot and S2251 assay. Varying plasminogen at fixed tPA and varying tPA at fixed plasminogen dose-response experiments were performed. V_0 (in S2251) and V_{FR} (in annular clot lysis assay) over component concentration were plotted using the primary axis. Equivalent plasmin activities were computed using equations derived from plasmin dose-response plots and were reported in U/mL in plots on the secondary axis (Figure 7A, 7B, 7D and 7E). At increasing plasminogen levels and a fixed 500 ng/mL tPA, S2251 assay reached its detection limit at ~29 µg/mL plasminogen. Conversely, V_{FR} from the annular clot lysis assay showed a clear increasing trend leveling-off at concentrations above 58.1 µg/mL. This indicates

that the annular clot lysis assay is a more sensitive candidate to determine plasminogen activity in plasma in the presence of endogenous or exogenous tPA.

At increased tPA levels and a fixed 58.1 μg/mL plasminogen, both V_0 and V_{FR} increased and showed a tendency to level off at higher tPA concentrations. Plasmin activities were compared across and within assays. As expected, in the absence of fibrin, the S2251 assay showed extremely low plasmin activity values converted using the standard curve and the equation derived in the plasmin dose-response experiment. The annular clot lysis assay showed two orders of magnitude larger ($P < 0.05$) plasmin activity values than those of S2251 at all tested groups for both varying tPA and varying plasminogen experiments. Within the annular clot lysis assay, plasmin activities showed significant differences across all groups ($P < 0.05$) when varying tPA. In experiments varying plasminogen, all groups showed significantly different plasmin activities compared to 2.9 μg/mL ($P < 0.05$) and all groups except 29.1 μg/mL showed significant differences compared to 5.8 μg/mL ($P < 0.05$). These results confirmed that the annular clot lysis assay could differentiate digestion rate or plasmin activities at a wide range of plasminogen or tPA levels. Overall, FLU200 decreased and leveled off at higher plasminogen or tPA levels (Figure. 7C and 7F). Importantly, the FLU200 of groups in these experiments were almost 3 times longer than groups with an equivalent V_{FR} in the plasmin dose-response experiment ($P < 0.05$). The extended lag phases in these samples were expected since the activation of plasminogen by tPA and the molecular interaction involving fibrin binding can contribute to elongated activation time prior digestion. These findings also demonstrated the capability of the annular clot lysis assay at picking up interplays between different fibrinolytic factors.

The tPA activation of plasminogen with S2251 was also run in the presence of soluble fibrinogen and a similarly low activation of plasminogen was observed (Suppl. Fig. 11). In general, tPA and plasmin(ogen) are key enzymes in the fibrinolytic pathway. Being capable of differentiating tPA and plasminogen levels in an unknown sample is an important assay feature. The annular clot lysis assay provides for a more versatile assessment of sample fibrinolytic potential compared to the S2251 assay. In addition, since tPA or alteplase is commonly used as a thrombolytic therapy for treating acute thrombosis events, the annular clot lysis assay could be conducted as a clinical pilot test to predict patient response to the thrombolytic therapy. Additional modifications to the annular fibrin clot assay can be made, for example, by including a patient's own plasma proteins, red blood cells and platelets to form labeled platelet-free or platelet-rich plasma clots and whole blood clots. In this way the annular clot lysis assay can be leveraged to potentially optimize the dosing strategy of a therapeutic prior to administering a treatment clinically.

The FITC-labeled annular clot lysis assay is a convenient method for a reliable assessment of sample fibrinolytic activity. The assay offers a real-time tracking of clot digestion where both a lag phase and a clot digestion rate can be identified and quantitatively compared. Based on these metrics, the present study has demonstrated the assay's capabilities of differentiating multiple fibrinolytic factors at physiological concentrations. In addition, the tagged clot substrate has long-lasting stability when stored at 4 °C for up to 8 weeks (Suppl. Fig. 12). This greatly expands its utility, especially under the fast-responding clinical setting as it does not need to be formed directly prior to use.

4. Conclusion

The annular clot lysis assay approaches a representative fibrinolytic process by utilizing a physiological relevant fibrin substrate with a concentration gradient-driven sample digestion. Formation of fibrin substrates at a known concentration enables the inter- and intra- test comparison of sample fibrinolytic potential. FITC labeling in the fibrin clot with a unique annular shape in the 96-well plate facilitate an easy-to-multiplex design to acquire fibrinolytic information of samples via a spectrometer (or fluorometer). By optimizing the fibrinogen: FhF ratio in the clotting mixture, the impact of FITC to fibrinogen conjugation on bulk fibrin properties such as clot strength and clot turbidity were minimized. Results demonstrated that the fibrinogen to FITC-fibrinogen ratios that mitigate deleterious effects associated with FITC tagging were at 10:1 for 3FhF, 30:1 for 7FhF, and 50:1 for 12FhF. SEM imaging results validated the similarity between 12FhF (50:1) and unmodified fibrinogen. Fibrinolytic activities of solutions containing different levels of plasmin were tested, both neat and physiologically relevant 12 FhF annular clot showed good limits of detection while neat 12FhF annular clots showed 19 times better sensitivity than its physiologically relevant counterpart. Testing a variety of samples against a standardized FITC-fibrin annular clot composition allows for direct comparison of fibrinolytic potential across diverse samples. It would be necessary to incorporate a subject's own plasma into the annular clot formation process to assess a subject's unique clot digestion profile.

Fibrinolytic activities of solutions containing plasminogen and tPA were further examined, the physiological relevant 12 FhF annular clot lysis assay could differentiate digestion at varying fibrinolytic component levels or varying fibrin-binding affinity. In addition, the physiological relevant clotting formulation exhibits clots with properties akin to native clots that make it feasible to test clot structure under alternate diverse clotting conditions. For example, clotting conditions can be adjusted to mimic pathological conditions and FITC labeled fibrin can be utilized as a reporter to determine effects on coagulation and fibrinolysis stemming from the pathologic conditions. The tunable fibrin clot substrate itself or as a base of a tunable synthetic blood clot can be used to mimic clinical clot or thrombi structures to provide insights into the treatment for thrombosis at specific patient conditions. For instance, annular clots can be made at varying fibrinogen levels to help predict therapeutic dosage for patient with fibrinogen deficiency or hyper-fibrinogen levels as were seen in COVID-19 patients [34,35]. The optimized FITC labeling fibrin(ogen) formula is also worth being introduced to studies that monitor FITC-fibrin digestion under a confocal microscopy because of its modest intensity and labeling homogeneity. Thrombolytic drug efficacy are usually examined in a ^{125}I-fibrinogen contained plasma clot [36,37]. The present assay is a better alternative for this type of study as FITC is a more accessible and less hazardous reporter compared to isotopic iodine.

Author Contributions

Ziqian Zeng: Conceptualization, Methodology, Investigation, Visualization, Formal analysis, Validation, Writing- Original draft preparation. **Tanmaye Nallan Chakravarthula:** Investigation. **Charanya Muralidharan**: Investigation. **Abigail Hall:** Investigation, Validation. **Amelia K. Linnemann:** Resources, Supervision. ***Nathan J. Alves****:* Conceptualization, Writing - Review & Editing, Supervision.

Conflict of Interest

The technology discussed here is patent pending with N. J. Alves and Z. Zeng as inventors. The authors confirm that there are no known conflicts of interest associated with this publication and there has been no significant financial support for this work that could have influenced its outcome.

Acknowledgments
This work was supported by the Department of Emergency Medicine at the Indiana University School of Medicine. Authors also acknowledge the support from Center for Diabetes Metabolic Diseases at IU school of medicine and IU Health 3D Innovations Lab.

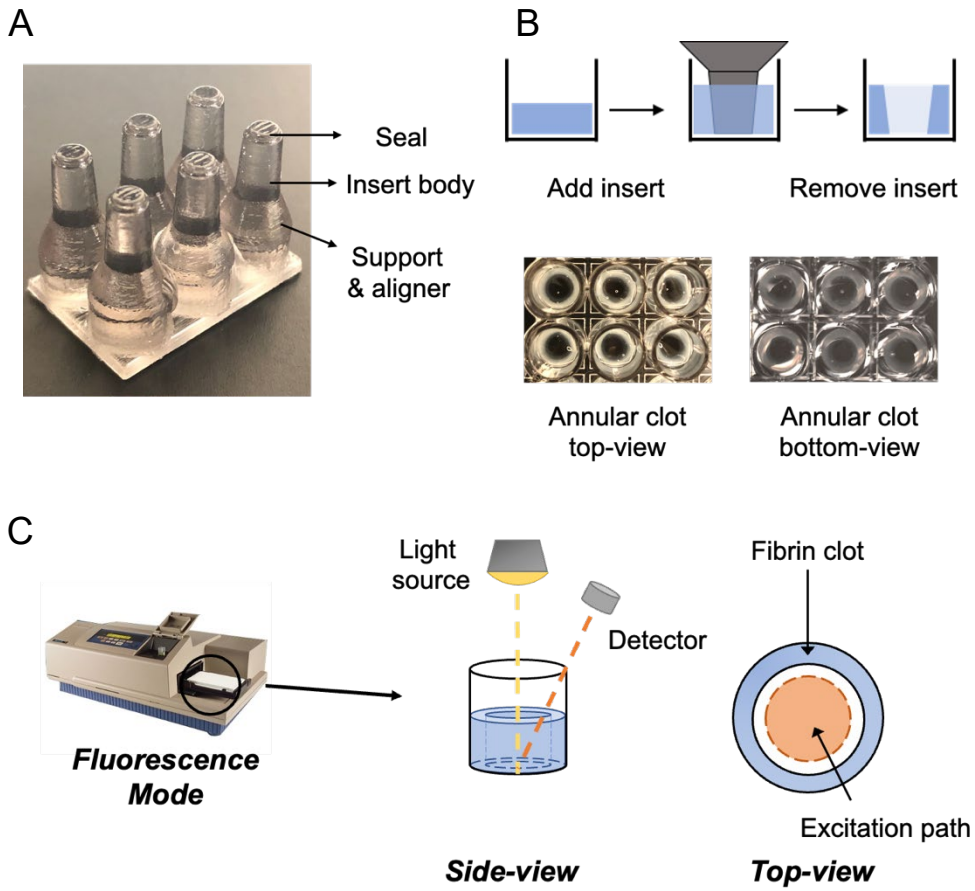

Figure 1: (A) The schematic of the 3D molding 3 X 2 insert and the printed product. (B) The schematic of annular clot formation in the well and the actual annular clot prepared by the 3 X 2 insert in the 96-well plate (C) Side and top views of the setup in the well. (2-column fitting image)

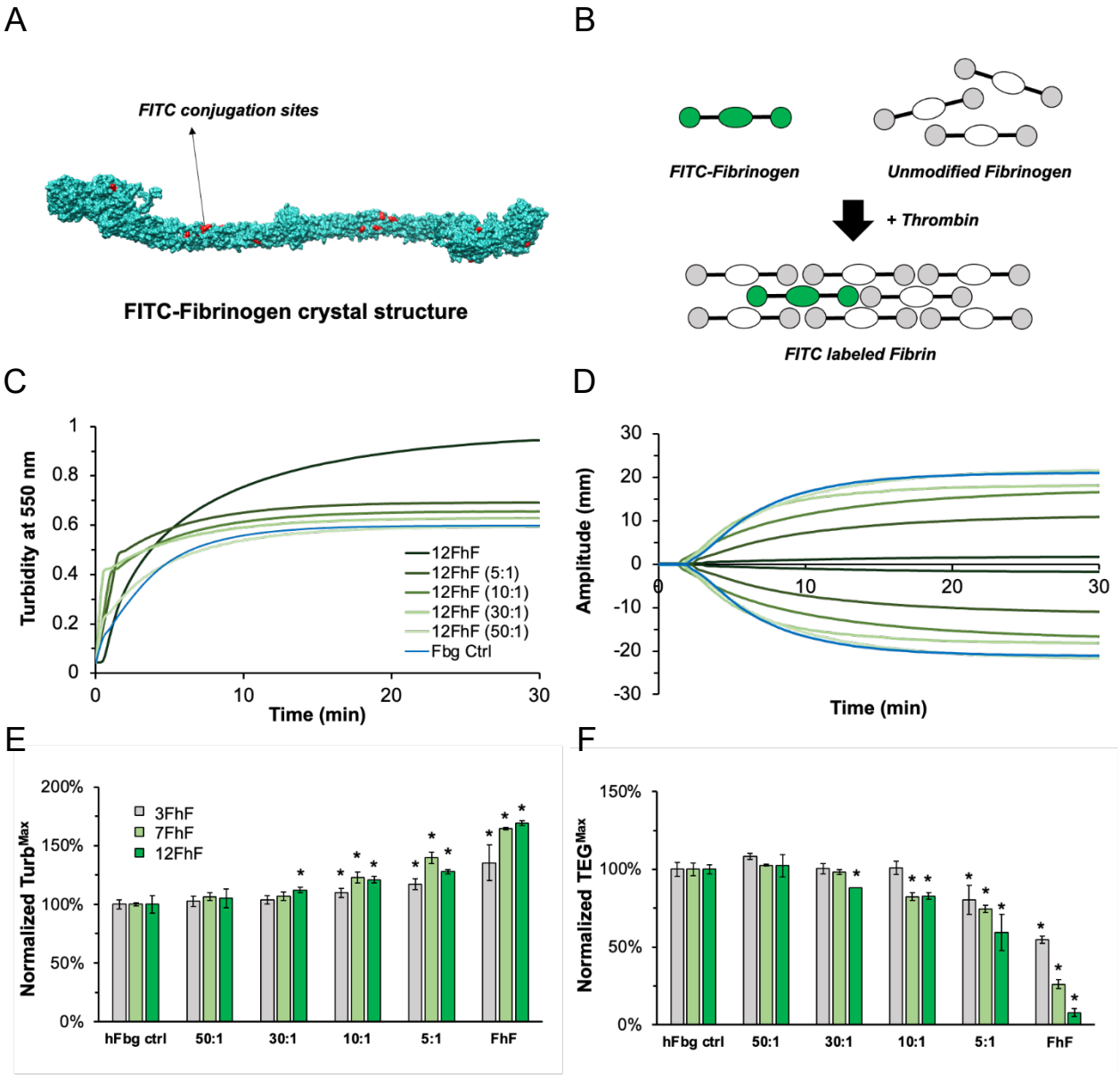

Figure 2: (A) Representative FITC conjugation sites on fibrinogen crystal structure displaying widespread FITC labels across the surface of fibrinogen. (B) Forming FITC labeled fibrin clot using thrombin-cleaved unmodified fibrinogen and FITC-fibrinogen mixture. Representative tracing curves of (C) turbidity assay and (D) TEG assay for varying 12FITC labeled human fibrinogen (FhF) levels in 12FITC-fibrin clot. (E) $Turb^{Max}$ and (F) TEG^{Max} (Maximum amplitude) of 3, 7 and 12- FITC-fibrin clots at different FhF levels were compared. Data were normalized by values of human fibrinogen control groups. * denotes significant differences (P value < 0.05) between FhF groups and hFbg ctrl group. (2-column fitting image)

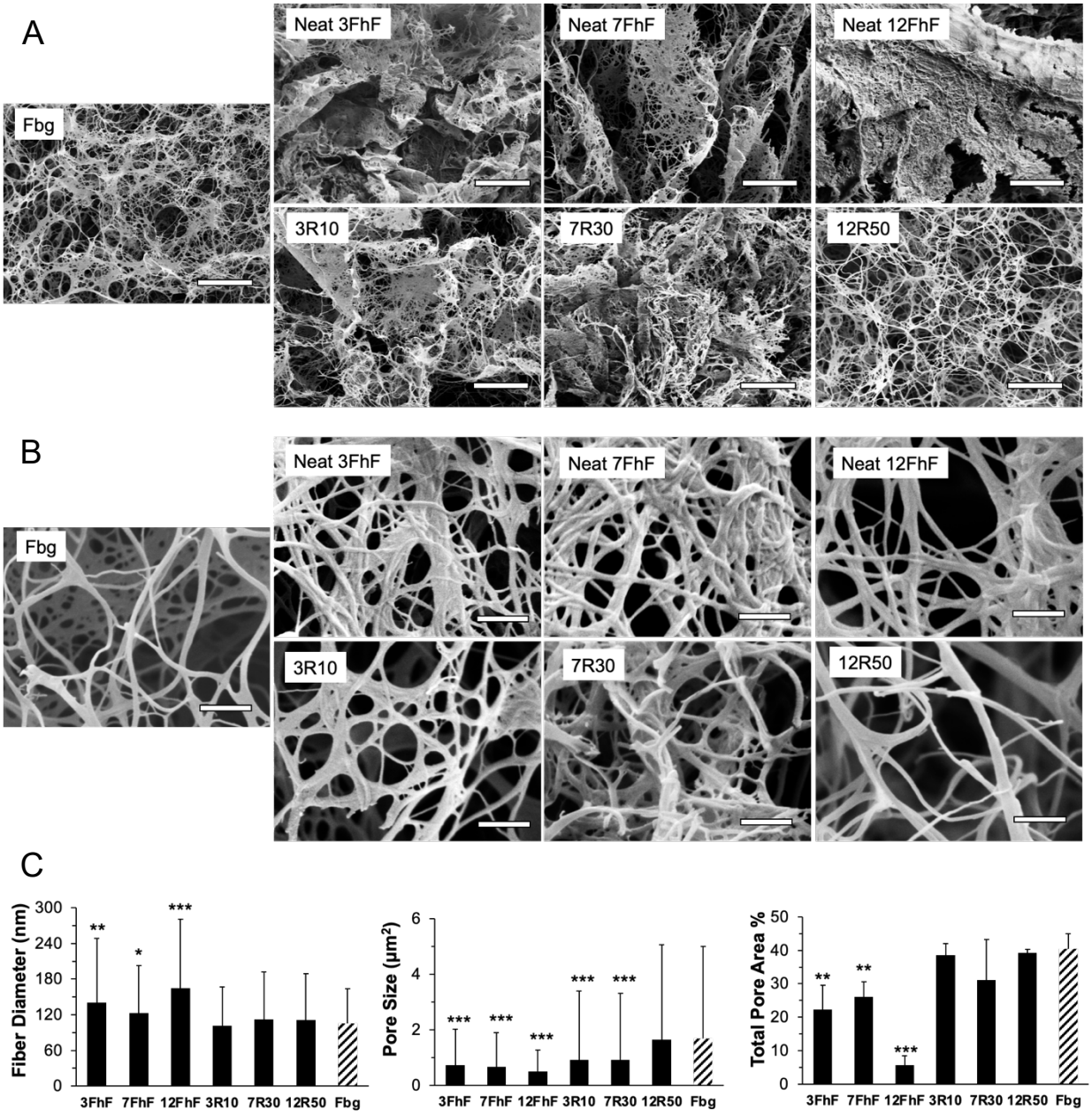

Figure 3: Representative SEM Images of FITC labeled human fibrin formed by neat and unmodified fibrinogen mixed 3, 7, 12- FITC-Fibrinogen at (A) 4,000X and (B) 35,000X. Scale bars were shown as 5 μm and 500 nm, respectively. Average fiber diameter (nm), average pore size (μm^2) and total pore area (%) were reported as bar plots and data were compared with unmodified fibrin controls using *, ** and *** denoting p values < 0.05, 0.001, and 0.0001. (2-column fitting image)

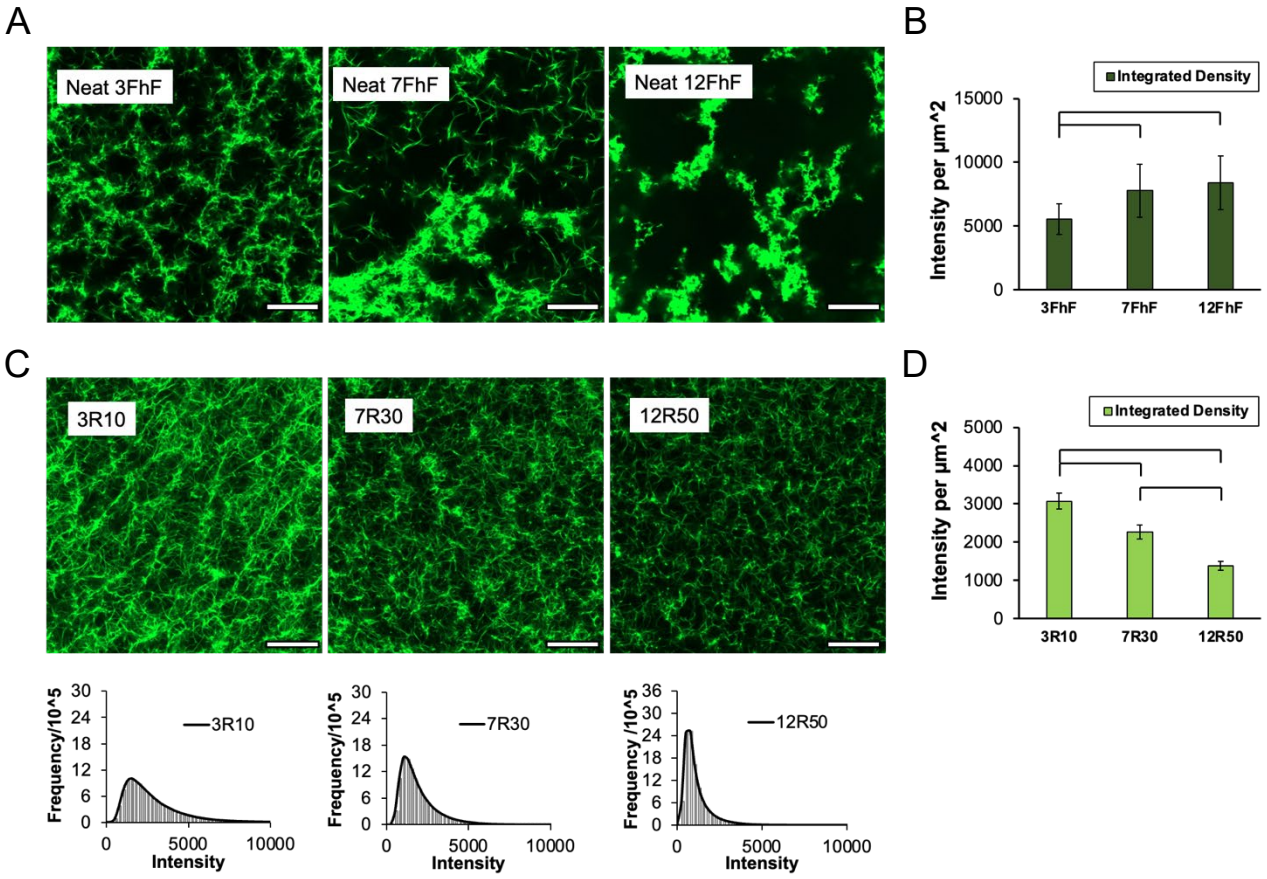

Figure 4: Representative confocal microscope images (40X objective with 1.5X digital zoom, excitation energy at 1%) of clots formed by (A) neat 3, 7, 12 - FhF, and (B) 3FhF (10:1), 7FhF (30:1) and 12FhF (50:1). Fluorescence intensity distribution were shown for physiologically relevant FhF clots. Integrated density was shown for (C) neat FhF and (D) physiologically relevant clots in bar plots with brackets denoting pairs of groups that exhibit significant differences ($P < 0.05$). Image brightness of 12FhF (50:1) clots were adjusted to enhance structure visualization. Scale bar = 20 µm. (2-column fitting image)

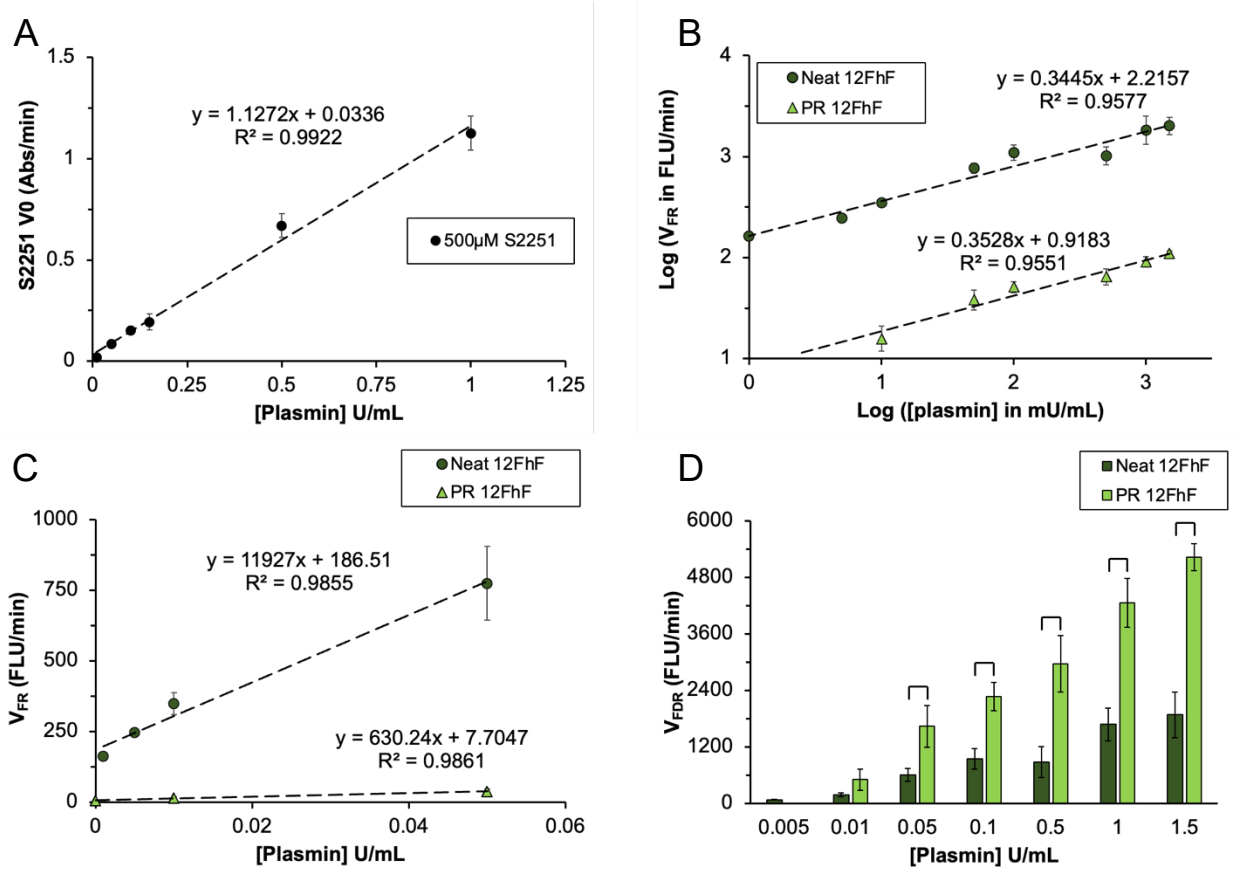

Figure 5: Plasmin dose-response curve by (A) initial velocity (V_0) in S2251 assay and (B) fluorescence release rate (V_{FR}) in neat and physiologically relevant (PR)- 12FhF annular clot lysis assay where data were shown at the double-logarithmic scale. (C) Analytical sensitivity determination curves of annular clot lysis assay by plotting data points below 0.05 U/mL plasmin. Analytical sensitivity of neat 12FhF and PR12FhF annular clots were 11927 and 630. (D) Fibrin degradation rate (V_{FDR}) at increasing [plasmin]. V_{FDR} of PR- and neat 12FhF were converted via multiplying their fluorescence release rates (FLU/min) by 50/12 and 1/12, respectively. All fluorescence tracing curves were shown in Suppl. Fig. 7 and 8. (2-column fitting image)

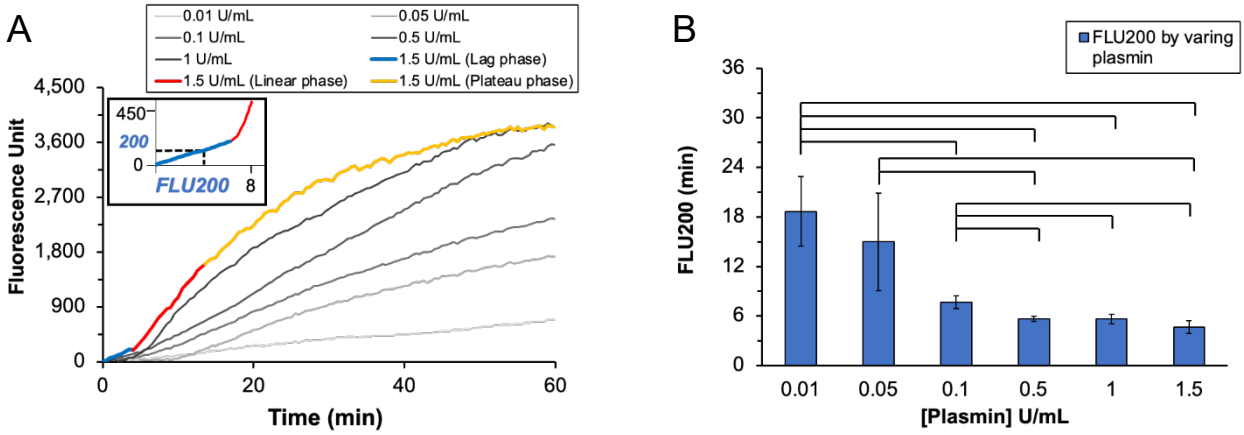

Figure 6: (A) Representative fluorescence release tracing curves of physiologically relevant (PR)-12FhF at varying [plasmin] and the derivation of FLU200 for PR-12FhF at 1.5 U/mL. (B) FLU200 for PR-12FhF over varying [plasmin]. Brackets denoting pairs of groups that exhibit significant differences ($P < 0.05$). (2-column fitting image)

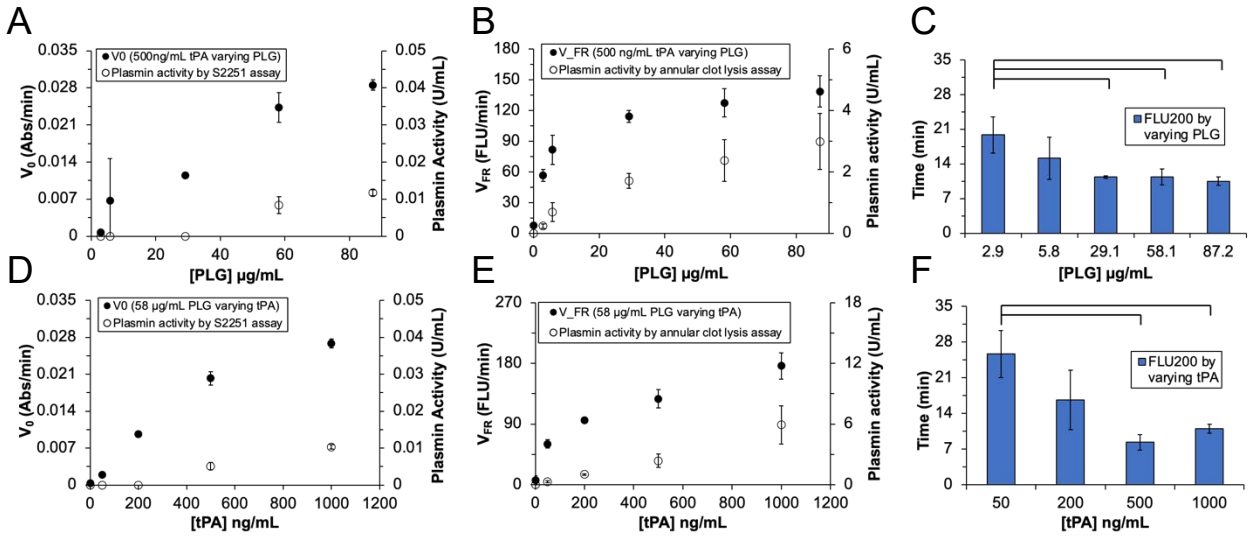

Figure 7: Digestion rates (primary axis, Abs/min or FLU/min) and plasmin activity (secondary axis, U/mL) by (A) fixed tPA and varying PLG in S2251 assay, (B) fixed tPA and varying PLG in PR-12FhF annular clot lysis assay (D) fixed PLG and varying tPA in S2251 assay and (E) fixed PLG and varying tPA in PR-12 FhF annular clot lysis assay. FLU200 by PR-12FhF were shown in bar plots at (C) varying PLG and (D) varying tPA experiments with brackets denoting pairs that have significant differences. Plasmin activities were converted by plugging the digestion rate values in linear regression equations derived in Figure.5. Plasmin activities were of two orders of magnitude faster in annular clot lysis assay compared to S2251 assay. Fluorescence tracing curves were shown in Suppl. Fig. 9 and 10. (2-column fitting image)

References

1 M. H. Prins and J. Hirsh, *Arch. Intern. Med.*, 1991, **151**, 1721.
2 C. P. M. Hayward, *Int. J. Lab. Hematol.*, 2018, **40**, 6–14.
3 C. Korninger, K. Lechner, H. Niessner, H. Gössinger and M. Kundi, *Thromb. Haemost.*, 1984, **52**, 127–130.
4 P. Toulon, *Int. J. Lab. Hematol.*, 2016, **38**, 66–77.
5 N. Mackman, R. E. Tilley and N. S. Key, *Arterioscler. Thromb. Vasc. Biol.*, 2007, **27**, 1687–1693.
6 M. W. Mosesson, *J. Thromb. Haemost.*, 2005, **3**, 1894–1904.
7 Q. Hao, B. R. Dong, J. Yue, T. Wu and G. J. Liu, *Cochrane Database Syst. Rev.*, , DOI:10.1002/14651858.CD004437.pub5.
8 G. A. Donnan, S. M. Davis, M. W. Parsons, H. Ma, H. M. Dewey and D. W. Howells, *Nat. Rev. Neurol.*, 2011, **7**, 400–409.
9 V. F. Tapson, K. Sterling, N. Jones, M. Elder, U. Tripathy, J. Brower, R. L. Maholic, C. B. Ross, K. Natarajan, P. Fong, L. Greenspon, H. Tamaddon, A. R. Piracha, T. Engelhardt, J. Katopodis, V. Marques, A. S. P. Sharp, G. Piazza and S. Z. Goldhaber, *JACC Cardiovasc. Interv.*, 2018, **11**, 1401–1410.
10 T. Urano, K. Sakakibara, A. Rydzewski, S. Urano, Y. Takada and A. Takada, *Thromb. Haemost.*, 1990, **63**, 082–086.
11 A. Ilich, I. Bokarev and N. S. Key, *Int. J. Lab. Hematol.*, 2017, **39**, 441–447.
12 T. Lisman, P. G. De Groot, J. C. M. Meijers and F. R. Rosendaal, *Blood*, 2005, **105**, 1102–1105.
13 W. B. Stubblefield, N. J. Alves, M. T. Rondina and J. A. Kline, *PLoS One*, 2016, **11**, e0148747.
14 J. Siudut, M. Grela, E. Wypasek, K. Plens and A. Undas, *J. Thromb. Haemost.*, 2016, **14**, 784–793.
15 M. E. Carr, L. L. Shen, J. A. N. Hermans and H. Chapel, 1977, **16**, 1–15.
16 J. Jespersen and T. Astrup, *Pathophysiol. Haemost. Thromb.*, 1983, **13**, 301–315.
17 N. J. G. L A Moroz, *Blood*.
18 E. Genton, A. P. Fletcher, N. Alkjaersig and S. Sherry, *J. Lab. Clin. Med.*, 1964, **64**, 313–320.
19 N. J. Mutch, L. Thomas, N. R. Moore, K. M. Lisiak and N. A. Booth, *J. Thromb. Haemost.*, 2007, **5**, 812–817.
20 V. Binder, B. Bergum, S. Jaisson, P. Gillery, C. Scavenius, E. Spriet, A. K. Nyhaug, H. M. Roberts, I. L. C. Chapple, A. Hellvard, N. Delaleu and P. Mydel, *Thromb. Haemost.*, 2017, **117**, 899–910.
21 G. Cesarman-Maus and K. A. Hajjar, *Br. J. Haematol.*, 2005, **129**, 307–321.
22 J. J. Wang, M. L. Baker, P. J. Hand, G. J. Hankey, R. I. Lindley, E. Rochtchina, T. Y. Wong, G. Liew and P. Mitchell, *Stroke*, 2011, **42**, 404–408.
23 Z. Zeng, M. Fagnon, T. Nallan Chakravarthula and N. J. Alves, *Thromb. Res.*, 2020, **187**, 48–55.
24 Z. Zeng, T. N. Chakravarthula and N. J. Alves, *J. Vis. Exp.*, 2020, **2020**, 1–7.
25 D. A. Armbruster and T. Pry, *Clin. Biochem. Rev.*, 2008, **29 Suppl 1**, S49-52.
26 J. H. Wu and S. L. Diamond, *Thromb. Haemost.*, 1995, **74**, 711–717.
27 T. W. Stief, R. Bünder, A. Richter, B. Maisch, H. Renz and J. Fareed, *Clin. Appl.*

Thromb., 2003, **9**, 211–220.
28 S. L. Diamond, *Annu. Rev. Biomed. Eng.*, 1999, **1**, 427–461.
29 D. V. Sakharov, J. F. Nagelkerkel and D. C. Rijken, *J. Biol. Chem.*, 1996, **271**, 2133–2138.
30 S. L. Diamond and S. Anand, *Biophys. J.*, 1993, **65**, 2622–2643.
31 T. Astrup and S. Müllertz, *Arch. Biochem. Biophys.*, 1952, **40**, 346–351.
32 J. Giedrojć, A. Stankiewicz, M. Walkowiak, M. Galar and M. Bielawiec, *Klin. Oczna*, 1996, **98**, 283–285.
33 S. M. Arcasoy and J. W. Kreit, *Chest*, 1999, **115**, 1695–1707.
34 M. Panigada, N. Bottino, P. Tagliabue, G. Grasselli, C. Novembrino, V. Chantarangkul, A. Pesenti, F. Peyvandi and A. Tripodi, *J. Thromb. Haemost.*, 2020, **18**, 1738–1742.
35 J. M. Connors and J. H. Levy, *Blood*, 2020, **135**, 2033–2040.
36 P. J. Burck, D. H. Berg, M. W. Warrick, D. T. Berg, J. D. Walls, S. R. Jaskunas, R. M. Crisel, B. Weigel, C. J. Vlahos, D. B. McClure and B. W. Grinnell, *J. Biol. Chem.*, 1990, **265**, 5170–5177.
37 J. C. Murciano, A. A.-R. Higazi, D. B. Cines and V. R. Muzykantov, *J. Control. Release*, 2009, **139**, 190–196.

Supplemental Material:
Fluorescently Conjugated Annular Fibrin Clot for Multiplexed Real-time Digestion Analysis

Ziqian Zeng [a,b], Tanmaye Nallan Chakravarthula [a,b], Charanya Muralidharan [c,d], Abigail Hall [a], Amelia K. Linnemann [c,d], Nathan J. Alves [a,b,c*]

[a] Department of Emergency Medicine, Indiana University School of Medicine, Indianapolis, IN
[b] Weldon School of Biomedical Engineering, Purdue University, West Lafayette, IN
[c] Departments of Biochemistry & Molecular Biology, Indiana University School of Medicine, Indianapolis, IN
[d] Department of Pediatrics, Indiana University School of Medicine, Indianapolis, IN

[*] Corresponding author:
Nathan J. Alves, PhD
Indiana University School of Medicine
635 Barnhill Dr. Rm. 2063
Indianapolis, IN 46202, United States of America
E-mail address: nalves@iu.edu (N.J. Alves).

Table of Contents:

Suppl. Table.1 Total pore area and fiber diameter of clot at different fibrinogen to 12FhF ratios

Clot formula	Pure 12FhF	12FhF R5	12FhF R10	12FhF R30	12FhF R50	Fibrinogen
Fiber diameter (nm)	***165 ± 115	***153 ± 83	***157 ± 114	*125 ± 79	111 ± 78	105 ± 59
Pore size (μm^2)	***0.5 ± 0.8	***0.9 ± 1.6	***1.1 ± 2.1	*1.3 ± 3.0	1.6 ± 3.4	1.7 ± 3.3
Total pore area	***5.7% ± 2.7%	*24.5% ± 7.5%	**28.0% ± 1.7%	39.2% ± 6.3%	39.3% ± 0.9%	40.4% ± 4.5%

Note: P values of groups comparing to the fibrinogen control group were determined by two-tailed unpaired t test, *** denotes P value <0.0001, ** denotes P value <0.001, * denotes P value <0.05.

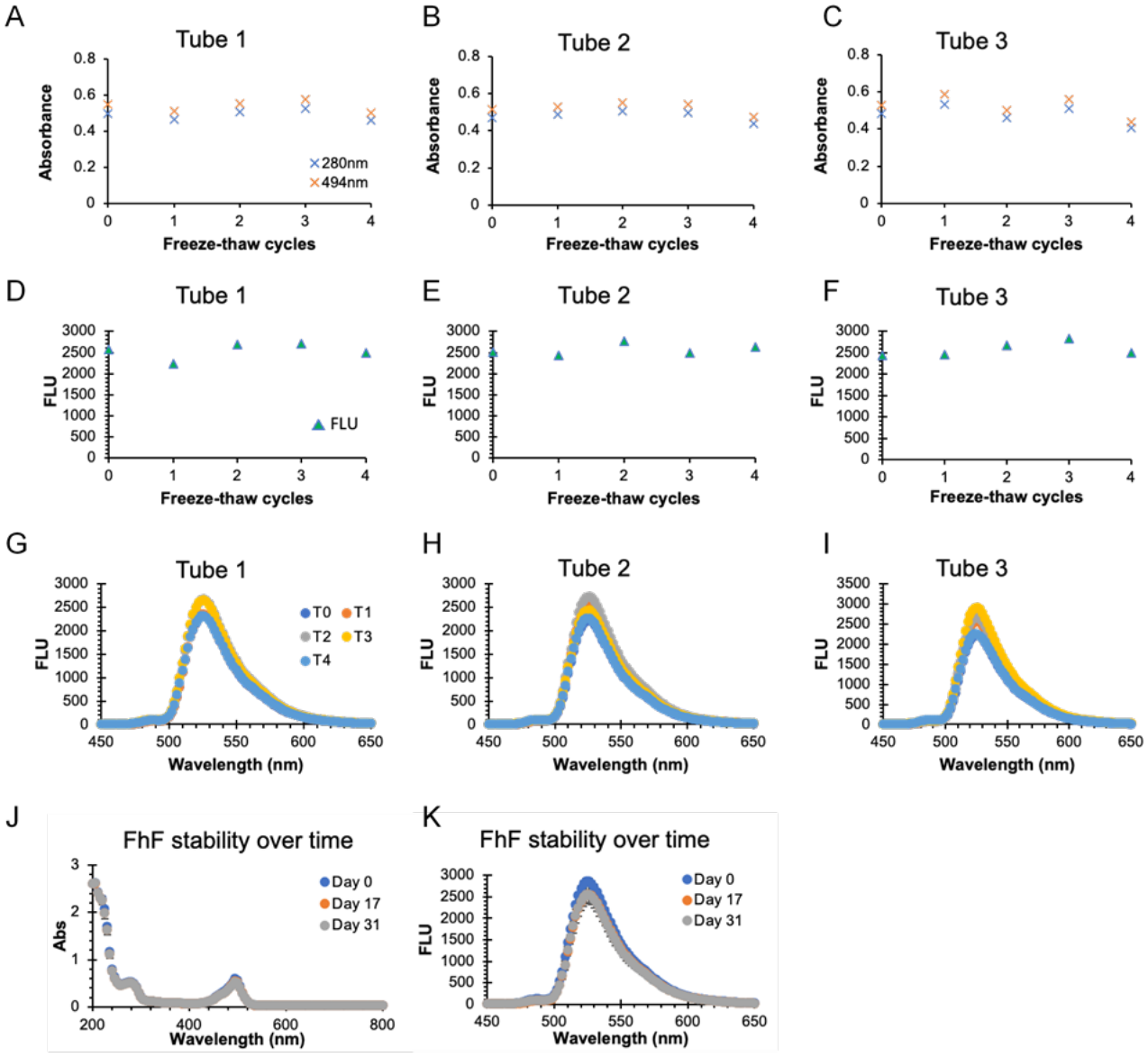

Suppl. Fig. 1: 12FITC-Fibrinogen (FhF) molecular and fluorescent stability after 4 freeze-thaw cycles. Three tubes of product were examined at (A, B, C) absorbance 280nm and 494 nm of stock aliquots at 20-fold dilution, (D, E, F) fluorescence endpoint Ex 495nm and Em 519 nm of stock aliquots at 400-fold dilution, and (G, H, I) additional fluorescent emission spectrum (Ex 495 nm, Em 450 - 650 nm, 400-fold dilution). No significant difference was found for product absorbance after 3 cycles (n=3, p_280 nm=0.1089, p_494nm=0.0897) and no significant difference were observed for emission spectrum as well as fluorescence endpoint after 4 cycles (n=3, p=0.2312). In addition, FhF aliquots were examined over storage time using the same metric. Both (J) absorbance spectrum and (K) fluorescence (Ex 495 nm, Em 450 - 650 nm, 400-fold dilution) showed consistent values over 31 days. This result indicates fluorescence intensity of FITC-Fbg product is stable after vigorous freeze-thaw cycles and storage.

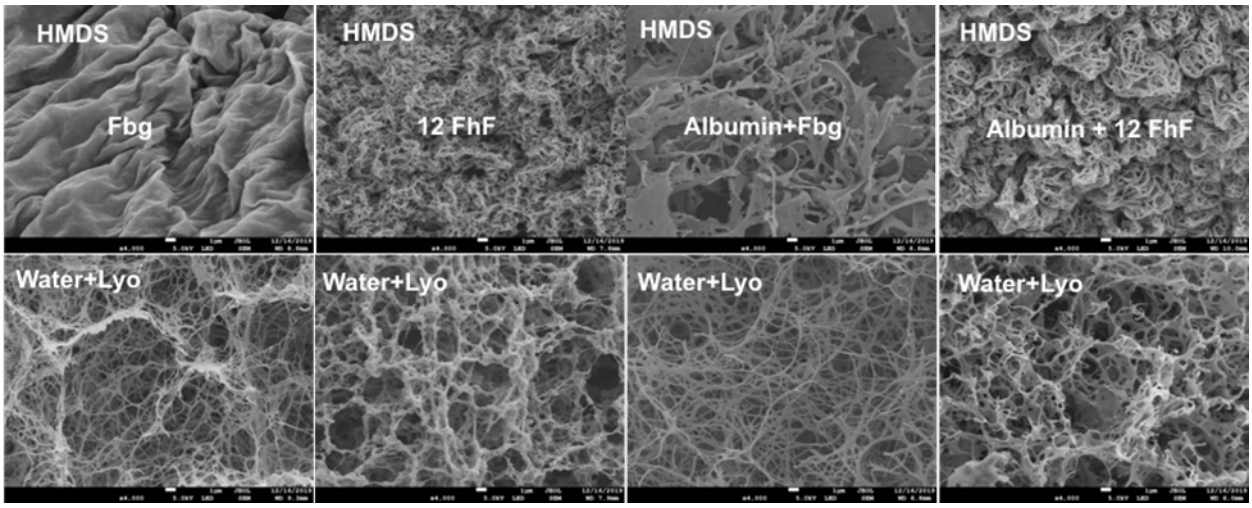

Suppl. Fig. 2: Representative SEM images (4,000X) were compared for ethanol-Bis(trimethylsilyl)amine (HMDS, Electron Microscopy Sciences Supplier, Hatfield, PA) (first row) and water-lyophilization dehydration methods (second row) of fibrin clots, which were formed by neat fibrinogen, neat 12FhF, Albumin + fibrinogen, and albumin + 12FhF. The HMDS method requires the washing of clot samples using a series of ethanol swaps at 30%, 50%, 70% and 100% (3 times), followed by a 50:50 ethanol to HMDS swap, and an overnight storage in 100% HMDS. However, the HMDS method results in clots that have 95% shrinkage while the lyophilization method offers a puffy dehydrated clot. Scale bar was shown as 1 μm in all images.

Suppl. Fig. 3: Identification of lysine / FITC conjugation sites on fibrinogen alpha, beta and gamma chains using mass spectrometry. One fibrinogen molecule has a pair of alpha, beta, and gamma chains. Available fibrinogen crystal structures (PDB entity sequence: 3GHG) are derived from the protein data bank for reference. The detailed protocol for fabricating FITC tagged fibrinogen molecules: Reacting human fibrinogen with a 200-fold excess FITC at RT for 24 hours and incubating for another 6 hours with the addition of doubled moles of fresh FITC to maximize the FITC conjugation on fibrinogen. The FITC-fibrinogen was then purified using 100kDa cutoff filter under 6 cycles of centrifugation to remove free FITC molecules. An average of 16 FITC per fibrinogen were identified through absorbance readings using the spectrometer method detailed in the main text. FITC-fibrinogen was then denatured in 8 M urea and digested by 1 µg trypsin/Lys-C protease mix for 4 hours at 37 C before dilution to 2 M urea overnight. Peptide sequences were examined using mass spectrometry. Data were subjected to post-translational modification (PTM) analysis using PEAKS Xpro to find FITC-lysine conjugation sites. Overall, PEAKS Xpro provided ~90% coverage of the fibrinogen protein and peptide sequences were included for analysis at less than 1% false discovery rate. The sum of all lysine residues in each pair are 43+36+34=113; wherein, mass spec covered lysine sites are 38+28+32=98, crystal structure known lysine sites are 16+4+5=25. Mass spec covered FITC sites are 16+6+5=27, and crystal structure known FITC sites are 4+4+5=13. Specifically, locations of these lysine are identified. Alpha chain (81% coverage, 16 sites): K89, K100, K148, K157, K227, K243, K322, K432, K437, K448, K467, K476, K558, K575, K602, K620. K238 is removed (since it had 390, but with a substitution in the peptide); Beta chain (83% coverage, 6 sites): K52, K77, K152, K163, K353, K367. K264 (missing 390 signatures though) and K426 (not full sequencing fragmentation) are removed; Gamma chain (90% coverage, 5 sites): K84, K101, K111, K146, K188. K199 is removed (missing 390, peptide has an AA substitution). Due to the lack of 100% coverage in both mass spec and available crystal structure a comprehensive identification of dominant lysine conjugation sites could not be further characterized. This data is, however; useful in demonstrating the diversity of conjugation sites indicating that there is some degree of conjugation variation even at saturating levels of FITC associated with a lysine conjugation technique of this nature.

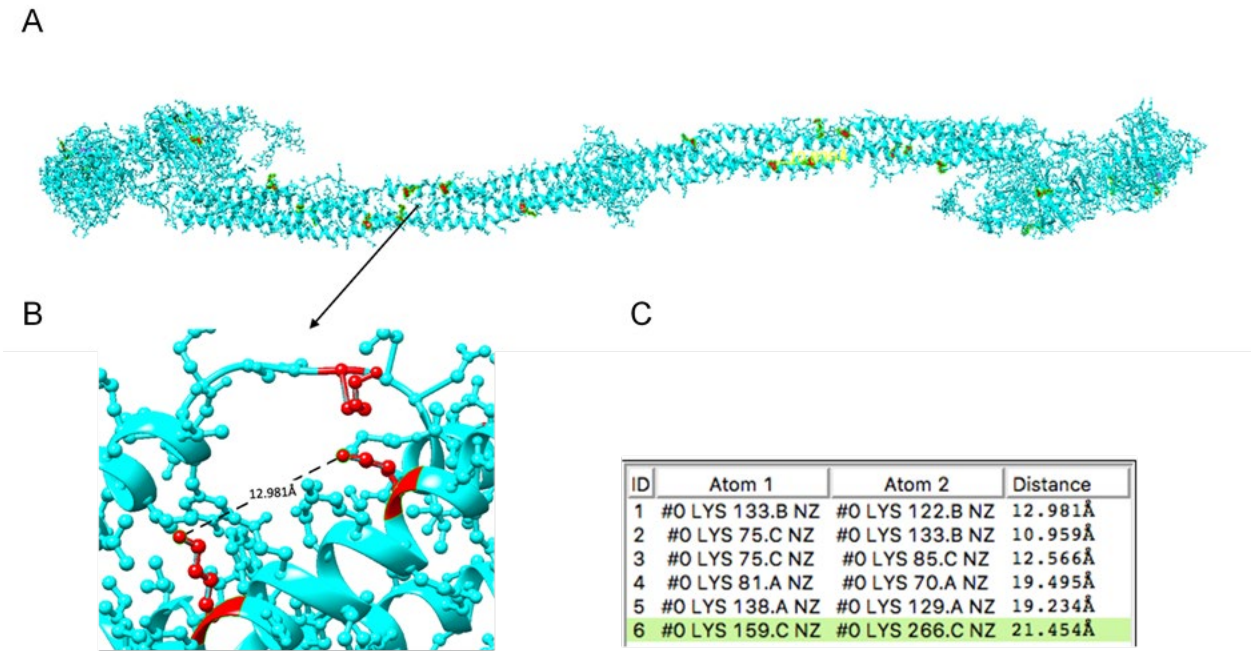

ID	Atom 1	Atom 2	Distance
1	#0 LYS 133.B NZ	#0 LYS 122.B NZ	12.981Å
2	#0 LYS 75.C NZ	#0 LYS 133.B NZ	10.959Å
3	#0 LYS 75.C NZ	#0 LYS 85.C NZ	12.566Å
4	#0 LYS 81.A NZ	#0 LYS 70.A NZ	19.495Å
5	#0 LYS 138.A NZ	#0 LYS 129.A NZ	19.234Å
6	#0 LYS 159.C NZ	#0 LYS 266.C NZ	21.454Å

Suppl. Fig. 4: (A) Fibrinogen crystal structure (PDB entity sequence: 3GHG, protein data bank) is shown in blue ribbon with identified FITC conjugation sites labeled in red. Despite an average of 16 FITC per fibrinogen calculated via absorbance, 54 lysine sites (27 sites in one set of fibrinogen alpha, beta, and gamma chain) were found to be accessible for FITC conjugation. This indicates that the conjugation reaction yields a heterogeneous FITC-fibrinogen mixture which can have different FITC amounts per fibrinogen or are products that have similar FITC amounts per fibrinogen but possess different combinations of FITC conjugation sites. The average 16 FITC per fibrinogen is most likely contributed by both scenarios. This is typical of non-site-specific conjugation techniques such as lysine-based labeling used here. In addition, only 52.8% of the fibrinogen crystal structure is known with the unknown part mostly belonging to the alpha C domain (representing 28 more possible FITC accessible lysine sites for conjugation). (B) shows a representative example of measuring the distance of adjacent FITC conjugation sites on available fibrinogen crystal structures using Chimera. In the known crystal structure of one set of the fibrinogen chains, 6 pairs (C) totaling 10 non-repeated conjugation sites were found to be within 20 angstroms of one another. Due to the proximity of these sites, the conjugation of one site within a pair likely reduces the probability of FITC subsequently conjugating the other one due to steric effects.

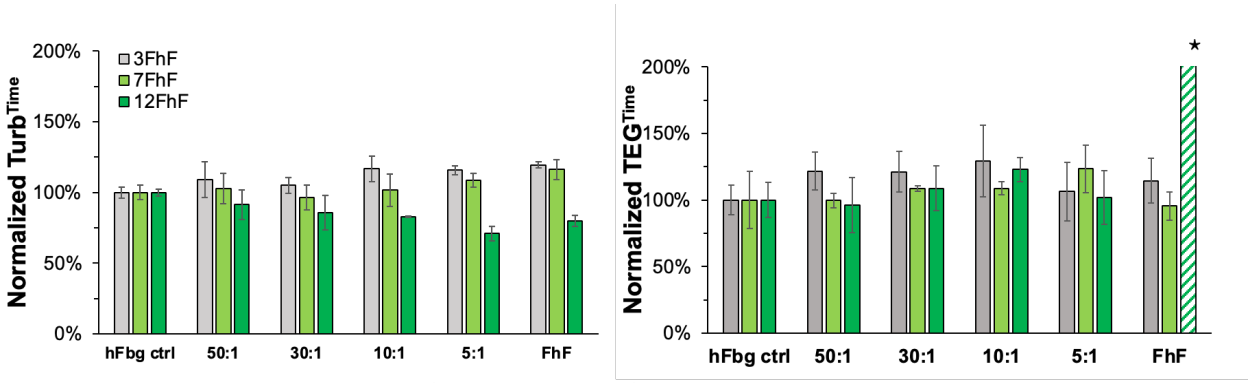

Suppl. Fig. 5: Comparing (A) $Turb^{Time}$ and (B) TEG^{Time} of FITC labeled human fibrin clots. Data were normalized by values of human fibrinogen control groups. ⋆ TEG^{Time} of neat 12-FHF is at 303%.

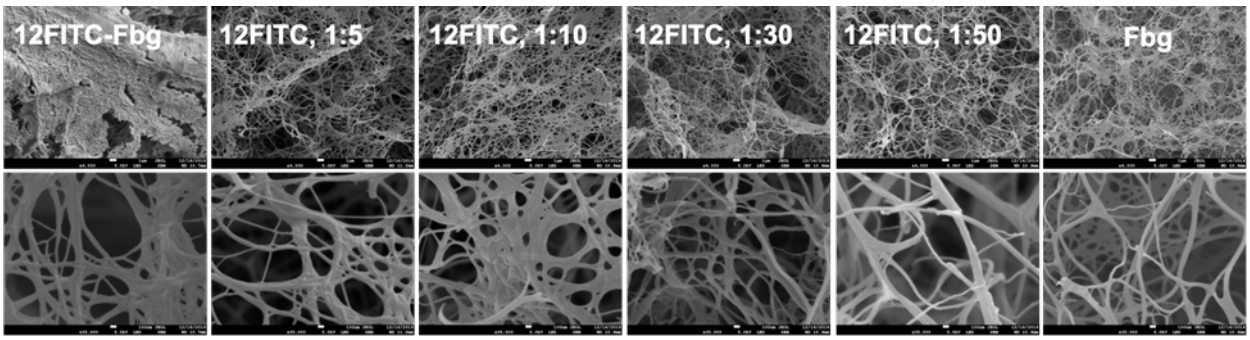

Suppl. Fig. 6: Representative SEM images of varying 12 FhF in fibrin. 4,000X (first row) and 35,000X (second row). Scale bars shown as 1 μm (first row) and 100 nm (second row).

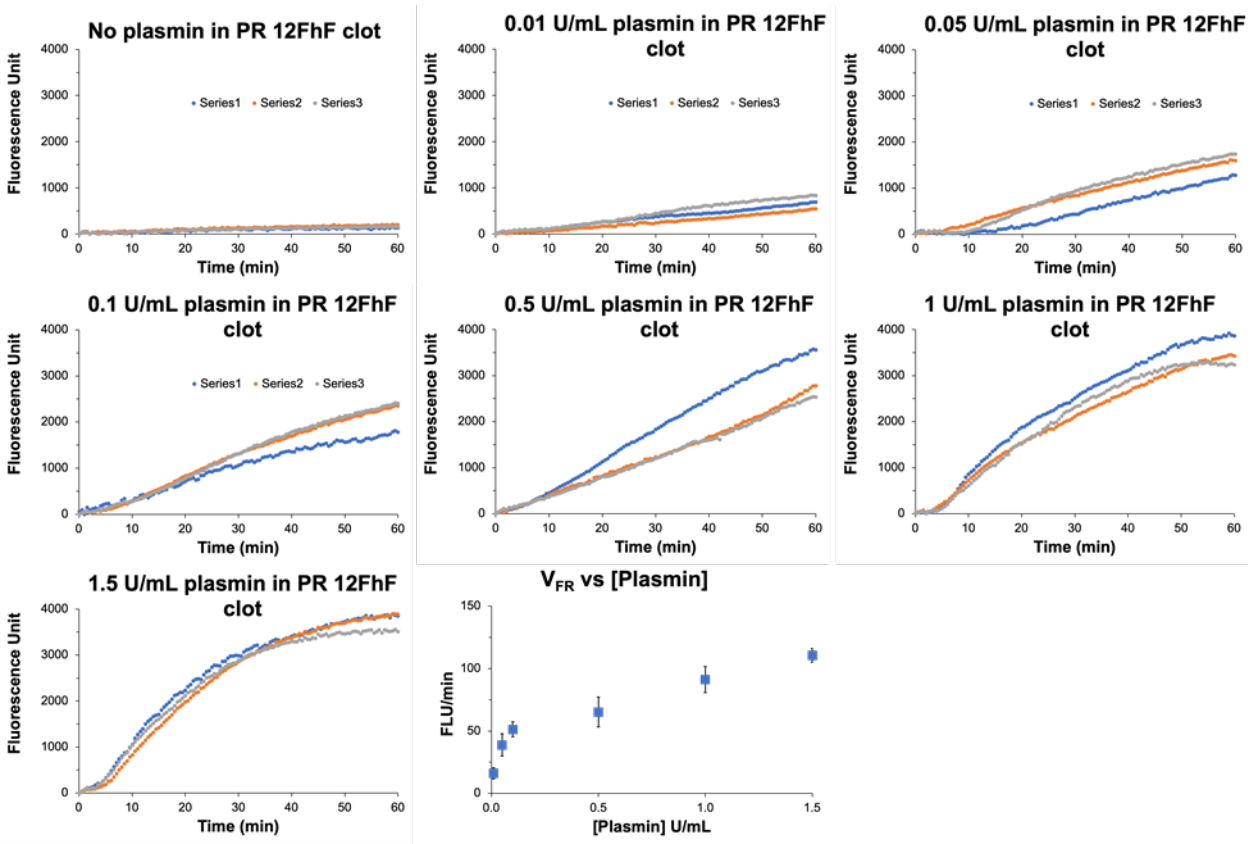

Suppl. Fig. 7: Fluorescence tracing curves of varying plasmin concentrations for digesting physiologically relevant 12FhF annular clots at 37 °C. The last figure shows V_{FR} (fluorescence release rate) over plasmin concentrations.

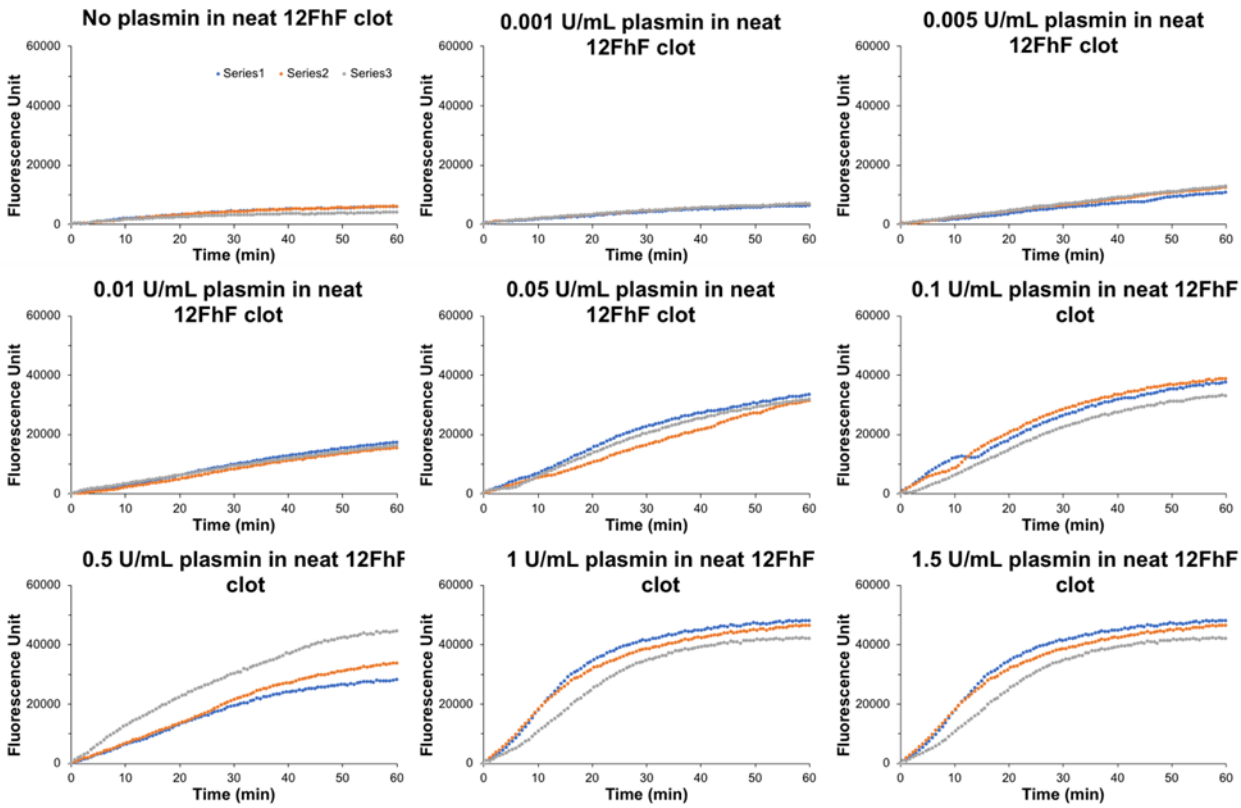

Suppl. Fig. 8: Fluorescence tracing curves of varying plasmin concentrations for digesting neat 12FhF annular clots at 37 °C.

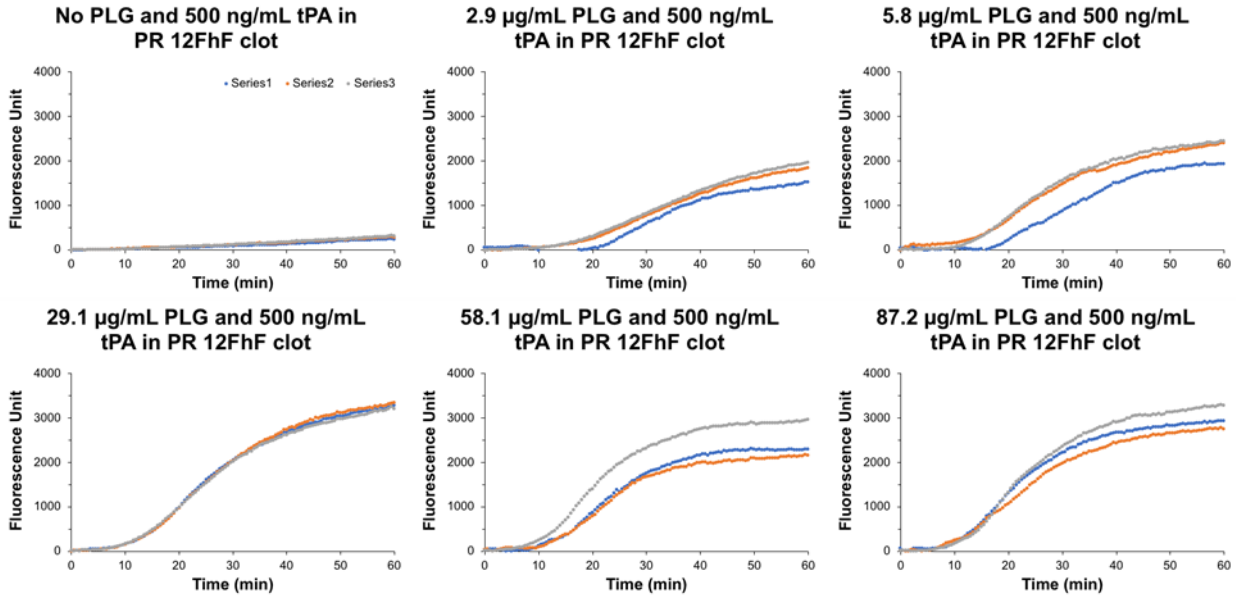

Suppl. Fig. 9: Fluorescence tracing curves of varying plasminogen concentration at fixed [tPA] for digesting physiologically relevant 12FhF annular clots at 37 °C.

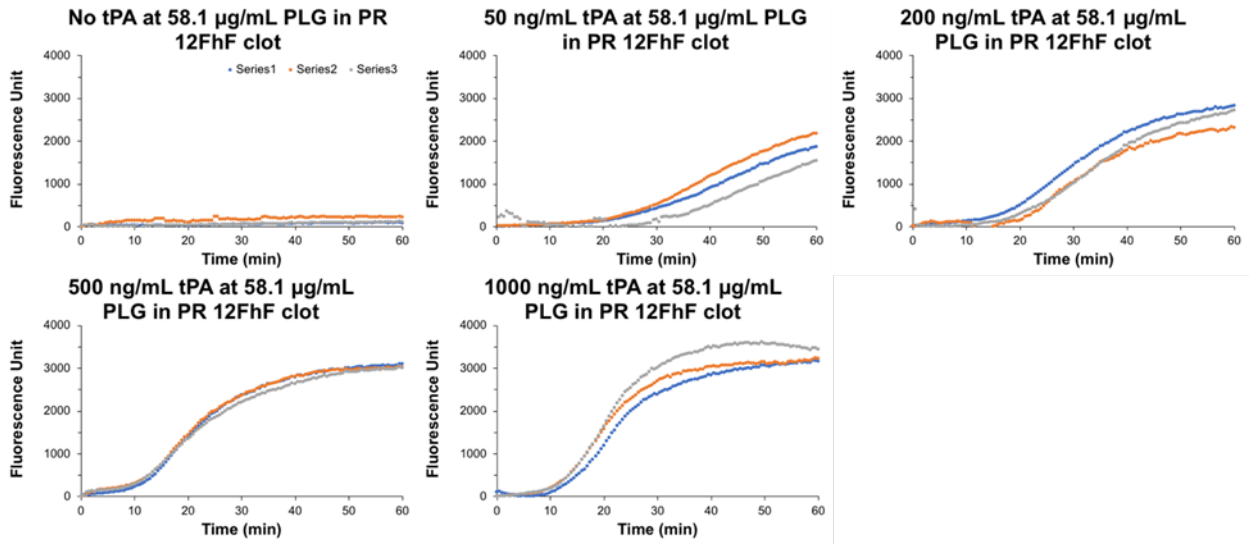

Suppl. Fig. 10: Fluorescence tracing curves of varying [tPA] at fixed plasminogen concentration for digesting physiologically relevant 12FhF annular clots at 37 °C.

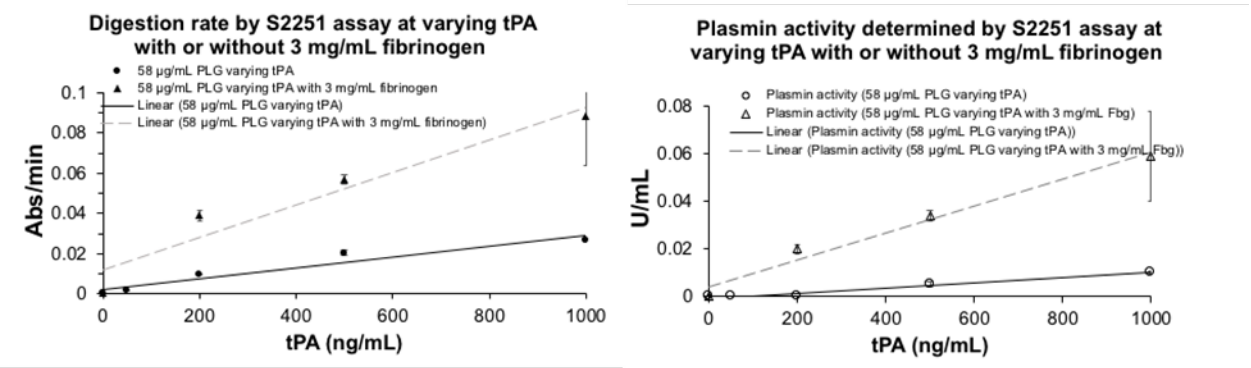

Suppl. Fig. 11: Comparing digestion rates (initial velocity, abs/min) at 405 nm by S2251 assay at varying [tPA] (0, 200, 500, 1000 ng/mL) with or without 3 mg/mL fibrinogen at 37 °C.

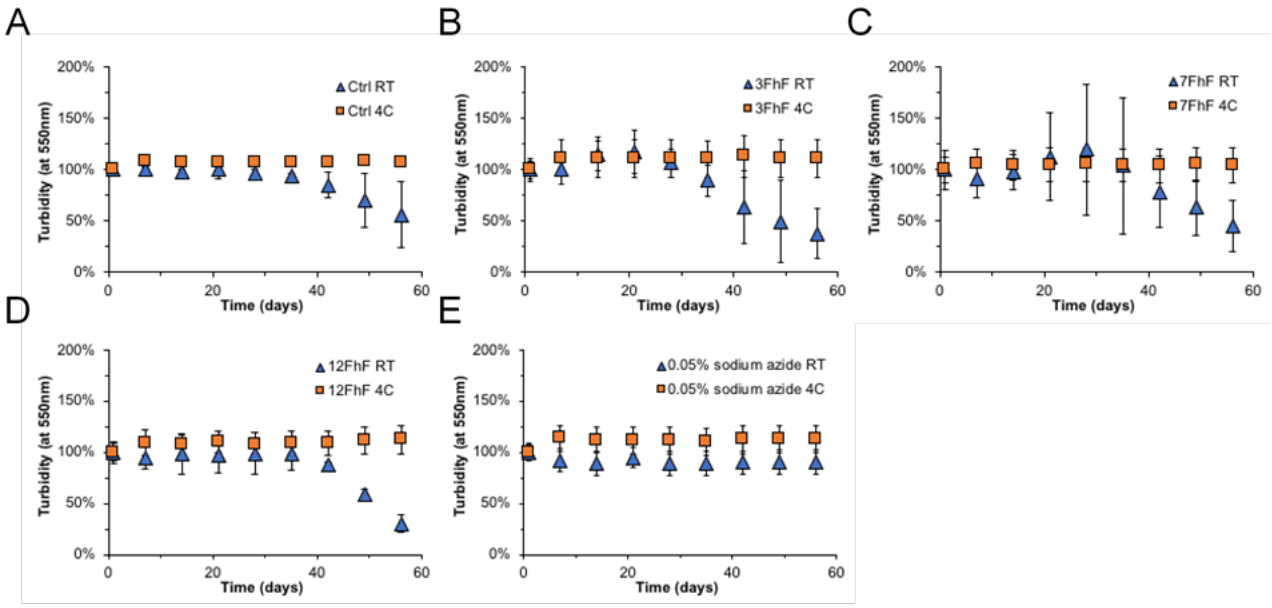

Suppl. Fig. 12: FITC-fibrin structural stability by clot turbidity (at 550 nm) over 8 weeks. Turbidity values were normalized by starting turbidity values of each sample. (A) Unmodified and (B, C, D) physiologically relevant 3, 7, and 12 FhF FITC-fibrin clots were formed in 96 well plates and stored at both RT and 4 °C to determine the long-term stability of the formed clots. Clot structures were monitored every week over 56 days through clot turbidity reads at 550 nm. Turbidity values tracked similarly across all groups. At RT, turbidity values started to decrease after 35 days and reached 30-50% of their starting turbidity at the end of the tested period. While 4°C turbidity values showed no overall changes ($P < 0.05$) for 3, 7, 12 Physiologically relevant (PR) FhF clots and no more than 8% overall changes ($P < 0.05$) for control clots throughout indicating a stable clot structure in all groups over 56-days. As there were no stabilizer agents specifically added to these samples, it is likely that the reduced turbidity over time observed at RT is due to bacterial growth. To test this, an additional untagged fibrin clot was stored in (E) 0.05% sodium azide and no reduction in turbidity was observed over 56-days. Long-lasting stability of a tagged clot substrate greatly expands its utility as it does not need to be formed directly prior to use.